Mechanisms of lava dome instability and generation of rockfalls and pyroclastic flows at Soufrière Hills Volcano, Montserrat

E. S. CALDER[1], R. LUCKETT[2], R. S. J. SPARKS[1] & B. VOIGHT[3]

[1] *Department of Earth Sciences, University of Bristol, Bristol BS8 1RJ, UK (e-mail: e.s.calder@open.ac.uk)*

[2] *British Geological Survey, Murchison House, West Mains Road, Edinburgh EH9 3LA, UK*

[3] *Department of Geosciences, Pennsylvania State University, University Park, PA 16802, USA*

Abstract: Between 3 January 1996 and 1 December 1998 at Soufrière Hills Volcano, Montserrat, there were 27 150 seismic signals attributable to rockfalls and pyroclastic flows. Large ($1–4 \times 10^6$ m^3) and major ($>4 \times 10^6$ m^3) dome collapses began to occur after the extrusion rate reached 2 m^3 s^{-1} and the lava dome exceeded 30×10^6 m^3 in volume. Large to major collapses occurred on 26 occasions and were usually associated with periods of elevated extrusion rate (6–13 m^3 s^{-1}), intense hybrid earthquake swarms and/or inflation–deflation cycles of crater-rim ground deformation. During these cycles, gas-rich pulses of magma, 140 000–320 000 m^3 in volume, were intruded into the dome and, soon thereafter, dome collapses from the headwalls of shear lobes were generated. Large dome collapses also occurred after 10 March 1998, when magma extrusion ceased, but these had no seismic precursors. These events represent structural failures from oversteepened canyon-like walls and were followed by intense degassing, suggesting that gas pressure build-up within the relict dome may have played some role. Rockfall counts and durations established from seismic data show variations that correlate with extrusion rate. Using pyroclastic flow runout and rockfall duration data as proxies for event magnitude, power law relationships between frequency (total number of events) and magnitude have been found. Seismic signals associated with rockfalls and pyroclastic flows commonly comprise both high-frequency and long-period components. Intense degassing from the dome is interpreted as the source for the long-period component. These results indicate that rockfalls and pyroclastic flows generated by dome collapse at Montserrat are not simply the result of passive dome failure, but are intimately related to discharge of pressurized gas and pulses of magma extrusion. Pyroclastic flows were usually sourced from lobe headwalls, where lava was hot and gas-rich and where fragmentation of the microvesicular andesite lava occurred more readily.

Lava dome eruptions commonly generate pyroclastic flows by collapse and disintegration of hot, microvesicular and usually crystal-rich lava. Pyroclastic flows generated in this manner are generally short-lived, occur in discrete pulses, and comprise blocks and lapilli of dense juvenile material. Relatively modest pyroclastic flows of this type have been observed in numerous eruptions: Mont Pelée in 1902 and 1929–1932 (Anderson & Flett 1903; Lacroix 1904; Perret 1937), Santiaguito in 1977 (Rose *et al.* 1977), Mount Unzen in 1990–1995 (Yamamoto *et al.* 1993; Nakada & Fujii 1993; Nakada *et al.* 1999), Colima in 1991 and 1998–1999 (Rodriguez-Elizarraras *et al.* 1991) and Merapi Volcano in 1984–1998 (Boudon *et al.* 1993; Abdurachman *et al.* 2000; Voight *et al.* 2000*a*, *b*). Such flows have been observed to travel a few to over 10 km from the vent, at speeds of as much as 60 m s^{-1}. Continued lava dome growth can generate pyroclastic flows repeatedly over a significant period of time, typically a few months to several decades (e.g. Mount Unzen, May 1991 to February 1995; Montserrat, March 1996 to at least December 2001; Bezymianny 1956–present). Yet, despite widespread occurrence, generation of these flows involves processes understood at only a basic level. Such flows arise from: (a) passive failure of unstable dome faces (e.g. Mellors *et al.* 1988; Ui *et al.* 1999); (b) failure of oversteepened lava-flow fronts or lava lobes (e.g. Sato *et al.* 1992; Yamamoto *et al.* 1993; Ui *et al.* 1999; Sparks 1997; Voight & Elsworth 2000); and (c) explosive expansion or diffusion of pore gas within the dome (Sato *et al.* 1992; Fink & Kieffer 1993; Voight & Elsworth 2000). Detachment of a significant mass of material from the dome can then generate a pyroclastic flow. The processes by which cascading debris transforms into a pyroclastic flow are not well understood. This phenomenon is generally attributed to the production of abundant fines by spontaneous disintegration of the lava: an inherent property of hot, crystal-rich lava containing pressurized gas in vesicles and connected pore space (Rose *et al.* 1977; Mellors *et al.* 1988; Sato *et al.* 1992; Voight & Elsworth 2000).

The ongoing eruption of Soufrière Hills Volcano, Montserrat, began on 18 July 1995 with a four-month period of phreatic activity centred in English's Crater (Fig. 1). In November 1995, an andesite lava dome started to grow within the crater and by late March 1996 the first small pyroclastic flows were generated by lava dome collapse (Young *et al.* 1998). High extrusion rates (2–6 m^3 s^{-1}) from July to September 1996 led to a series of large dome collapses, culminating in a magmatic explosive eruption on 17 September (Robertson *et al.* 1998). Dome extrusion continued and, as English's Crater was open to the east, until March 1997 all pyroclastic flows were confined to the Tar River valley (Fig. 1). Subsequent overtopping of the southern, western and northern parts of the crater wall led to formation of significant deposit fans on all sides of the dome (Fig. 1). A detailed account of the pyroclastic flow chronology can be found in Cole *et al.* (2002). Two series of Vulcanian explosions (Druitt *et al.* 2002*b*) occurred in August and September–October 1997, and a large debris avalanche and dome collapse occurred on 26 December 1997 (Sparks *et al.* 2002) removing about 55×10^6 m^3 of the lava dome and volcanic edifice. Dome extrusion continued until around 10 March 1998, at which time the total amount of magma erupted since 1995 was 300×10^6 m^3 dense rock equivalent (DRE). With cessation of magma extrusion, seismic activity decreased. A major dome collapse on 3 July 1998 marked the onset of a series of collapses and explosions (Norton *et al.* 2002) although no renewed extrusion was apparent. In November 1999, after 20 months of residual activity, a second phase of lava extrusion commenced. This paper deals with the period November 1995, when lava extrusion commenced, to November 1999.

During the eruption of Soufrière Hills Volcano, pyroclastic flows have been generated by a number of different mechanisms (Cole *et al.* 1998, 2002): (1) pyroclastic flows caused by the collapse of the lava dome; (2) surge-derived pyroclastic flows (Druitt *et al.* 2002*a*); and (3) pyroclastic flows formed by collapse of vertically directed eruption columns (Druitt *et al.* 2002*b*; Clarke *et al.* 2002; Norton *et al.* 2002). Activity has been dominated by dome-collapse pyroclastic flows, herein simply referred to as *pyroclastic flows*. The behaviour of these flows, and the nature of their respective deposits, are largely similar to those of dome-forming eruptions elsewhere (Anderson & Flett 1903; Yamamoto *et al.* 1993; Boudon *et al.* 1993; Cole *et al.* 2002). During the period November 1995 to December 1999, over 165×10^6 m^3 of rock debris was shed from the dome as pyroclastic flows, the deposits of which inundated over two-thirds of the volcano's flanks (Fig. 1).

Understanding dome stability and the mechanisms of pyroclastic flow formation are key objectives in volcanology. Previous investigations (Mellors *et al.* 1988; Sato *et al.* 1992; Yamamoto *et al.* 1993; Ui *et al.* 1999) were based on detailed photographic

DRUITT, T. H. & KOKELAAR, B. P. (eds) 2002. *The Eruption of Soufrière Hills Volcano, Montserrat, from 1995 to 1999.* Geological Society, London, Memoirs, **21**, 173–190. 0435-4052/02/$15 © The Geological Society of London 2002.

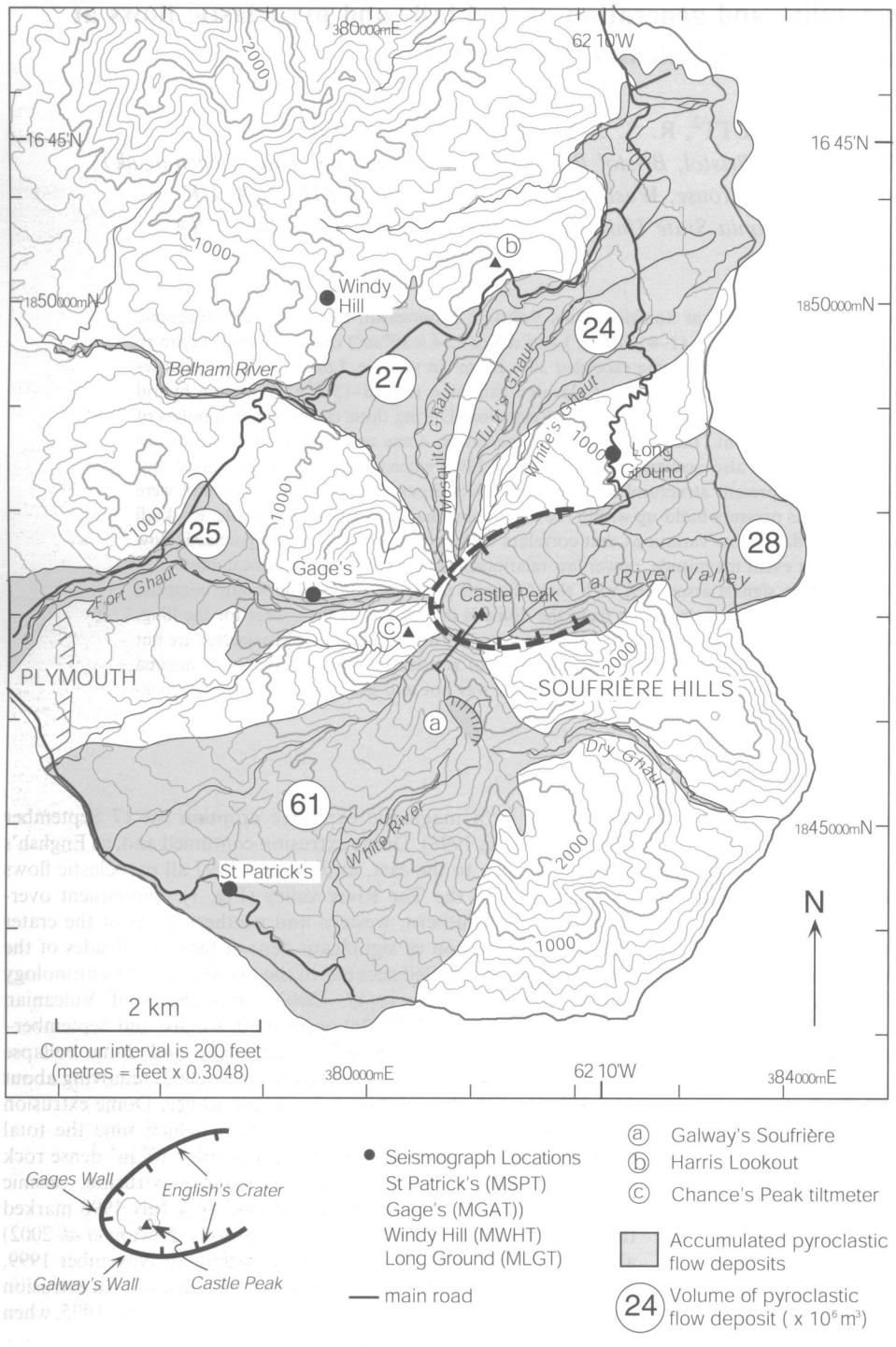

Fig. 1. Map of southern Montserrat with distribution of total accumulated (November 1995–March 1998) pyroclastic flow deposits. Topography exerted a major control on flow paths and, therefore, on the spatial development of the depositional fans over time (Cole *et al.* 2002). The volumes ($\times 10^6$ m^3) of pyroclastic flow material accumulated within each of the main drainage systems are given. The deposit volumes within the Tar River and White River valleys are underestimates of the actual volumes discharged in those directions, as many of the flows there entered the sea. Key locations, such as the positions of selected seismic stations (black dots) and the Chance's Peak tiltmeter, are given. English's Crater and the locations of Galway's Wall and Castle Peak are shown in the bottom left-hand corner. The section line through English's Crater wall marks the position of the section in Figure 6c.

documentation of collapsing lava lobes and their spontaneous disintegration. Theodolite measurements of the advancing lobes at Mount Unzen Volcano constrained critical overhanging angles at which failure and detachment occurred (Yamamoto *et al.* 1993). Tilt and seismic precursors to dome collapse were recognized at Merapi Volcano (Voight *et al.* 2000*a*, *b*). In this paper, we consolidate data from several monitoring methods used at the Montserrat Volcano Observatory (MVO) to examine the mechanisms of dome collapse and pyroclastic flow generation. Measurements of magma extrusion rates, crater-rim ground deformation, and seismicity associated with the Montserrat pyroclastic flows have been an integral part of MVO monitoring. We investigate how these processes influence dome instability and, subsequently, pyroclastic flow generation, thus enabling some advances in understanding of the causative mechanism of dome collapses.

Lava dome instability

Dome-collapse phenomena

Relatively simple 'gravitational' collapse of lava domes commonly generates pyroclastic flows that are referred to as 'Merapi type' flows (Escher 1933; Voight *et al.* 2000*a*). These represent the large-scale end-member of the spectrum of lava-dome-collapse phenomena. Collapses of the Soufrière Hills lava dome range from conventional lava block rockfalls, through small, pyroclastic flows to major collapses involving as much as 55×10^6 m^3 of material.

Rockfalls represent the smaller-scale end-member of collapse phenomena, and range from assemblages of discrete blocks (sometimes up to 20 m diameter or more) that roll, bounce and slide downhill, to avalanches of blocks that produce substantial volumes

of fine ash. Rockfalls rarely travel far beyond the base of the talus apron 0.5–0.8 km from the dome summit, but they can involve moderately large quantities of material. On the basis of visual observations, rockfalls can be distinguished as either (1) passively generated, occurring during periods of little apparent growth, and relatively low activity, or (2) actively generated, occurring during periods of more intense, continuous or semi-continuous rockfall activity associated with new growth, or with recent changes in the locus of active growth. Passively generated rockfalls occurred typically as isolated events on inactive flanks. Relatively little elutriation of fine ash is produced during these events. Ash appears to be mostly surface ash kicked up by blocks rather than fresh ash formed by comminution and block disintegration. Small, gently convecting clouds that formed above passive rockfalls rapidly lost coherency and deteriorated into diffuse, laterally drifting clouds that travelled only a few hundred metres. Many of these rockfalls were initiated by discrete, falling blocks that descended whole with little fragmentation, remobilizing talus en route and initiating slow grain flow. In contrast, actively generated rockfalls are derived from active or rapidly growing parts of the dome. Associated ash clouds commonly convected vigorously and rose as small coherent plumes for 300–1000 m (Fig. 2a). This hot, more buoyant ash was formed by fragmentation during avalanching. These actively generated rockfalls graded into pyroclastic flows when larger volumes of similar material collapsed. During the period of magma extrusion, from November 1995 to March 1998, 20–140 rockfalls were commonly generated every day.

Pyroclastic flows are distinguished from rockfalls by their larger size, longer runouts ($\gg$0.5 km), greater production of fine ash and appreciable buoyant hot ash clouds. Qualitatively, pyroclastic flows form when there is a larger proportion of ash produced by rapid, spontaneous disintegration of the collapsing dome material (Sato *et al.* 1992). Pyroclastic flows comprise a *basal avalanche* or *block-and-ash flow* of dense blocks, lapilli and ash and an overriding, dilute *pyroclastic surge* component. The surge component of these flows is, at least in part, derived by elutriation from the underlying avalanche (Fig. 2b). The basal avalanche is generally incandescent and poorly sorted (Calder *et al.* 1999; Grunewald *et al.* 2000; Cole *et al.* 2002). The pyroclastic surges had a significant lateral component of motion, but those associated with small pyroclastic flows were commonly very weak: the upper, buoyant portions of the surge are referred here to as *ash plumes* (Fig. 2c). These were generated sequentially along the flow path and rose a few hundred metres to several kilometres or more during large collapses (Bonadonna *et al.* 2002), producing high-rising thermals (Woods & Kienle 1994).

In practice, there is a continuum of collapse phenomena, and thus for small events it is difficult to define rigorously whether a particular event is a rockfall or pyroclastic flow (e.g. Fig. 2a). Between March 1996, when the first pyroclastic flows were produced, and February 1998, small (<1 km) pyroclastic flows occurred on an almost daily basis. Deposit volumes were about 10^3–10^4 m^3 for small pyroclastic flows and 10^4–10^6 m^3 for typical, medium-sized (runouts of 1–4 km) pyroclastic flows, such as that of 12 May 1996, which travelled 2.9 km down the Tar River valley and reached the sea (Cole *et al.* 2002).

Large dome collapses on Montserrat, defined here as those with deposit volumes 1–4 $\times$ 10^6 m^3, occurred on 18 occasions throughout the eruption (Table 1). Eight dome collapses had deposit volumes >4 $\times$ 10^6 m^3 and are defined as major dome collapses. Large to major collapses represented significant events in the eruption chronology and therefore were periods when the MVO was on heightened alert. They occurred as discrete single-pulse events (<5 minutes' duration) or as sustained events, where a major portion of the dome collapsed over a period of a few minutes to as much as several hours (Table 1). During the longer collapse episodes (e.g. 11 April 1997, 180 minutes; 3 August 1997, 120–150 minutes), retrogressive failures excavated spoon-shaped cavities as much as 200 m deep in the dome. On collapse, each large slice of dome generated discrete, large-volume, energetic flow pulses producing discrete peaks in seismic energy. These main flow pulses were to some extent masked by the quasi-continuous generation of smaller-scale rockfalls that preceded, accompanied and followed large collapses. Deposit volumes of these flows ranged between 1 $\times$ 10^6 m^3 and 55 $\times$ 10^6 m^3 (Table 1), with runout distances from 3 km to 6.7 km.

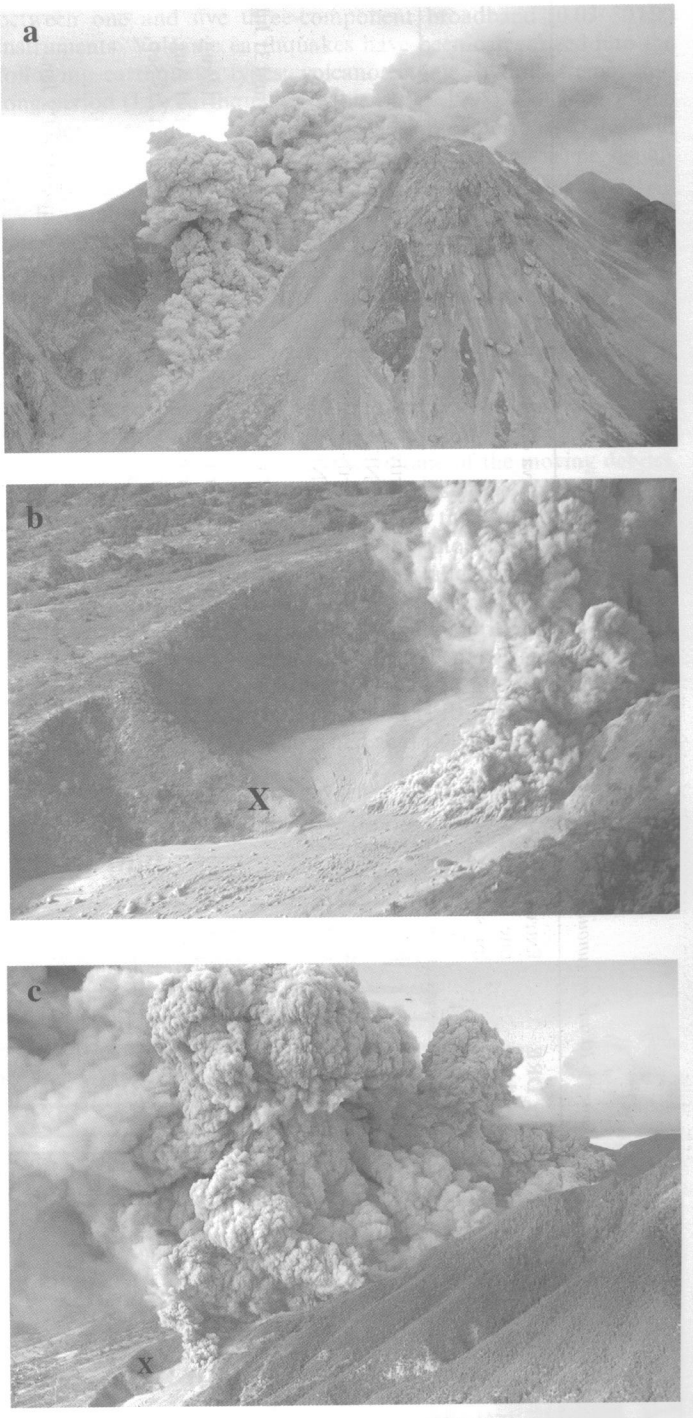

Fig. 2. (**a**) The Soufrière Hills lava dome in February 1997. The upper third of the dome is composed of coherent, blocky andesitic lava, with the lower two-thirds being an apron of loose talus. A rockfall is seen travelling down the eastern side of the dome into the upper reaches of the Tar River valley. Rockfalls sourced from active growth areas on the dome tended to generate small, but coherent, ash plumes such as the ones shown in this photograph. (**b**) A pyroclastic flow in the White River valley in November 1997. The flow is confined, with a low snout and overriding ash clouds. The average velocity was 8–16 m s^{-1}. (**c**) The same flow as shown in (b), but a few seconds earlier (note the position of the flow front relative to the valley corner 'X'. The buoyant ash plumes generated above the flow dominate the scene, while the front of the basal avalanche is rarely observed. Ash plumes rise several hundred metres to 14 km in the largest collapse events. The scale of the thin basal avalanche, relative to the several-kilometre-high overriding ash plumes, is one of the most striking features.

Table 1. *Summary of large to major dome collapses of the eruption, as defined by deposit volumes >10^6 m^3 or runout distances over 3 km*

Collapse date	Deposit volume ($\times 10^6$ m^3)	Volume calculation based on	DRE collapse volume ($\times 10^6$ m^3)	Hybrid swarms	DRE dome volume ($\times 10^6$ m^3)	Extrusion rate (m^3 s^{-1})	Percentage of dome collapse	Collapse duration (min)	Relation to lava dome growth
29 Jul. 96*	2.8/3.0[1]	Deposit map	2.3	Y	24.9	5.2	9.2	180	Occurred shortly after switch in dome growth, new lobe directed to NE
31 Jul. 96*	~1.0	Deposit estimate	0.8	Y	~23.0	4.6	3.5		Occurred shortly after switch in dome growth, new lobe directed to NE
4 Aug. 96*	~3.0	Scar/fan survey	2.3	Y	~23.0	2.1	10.0		
11 Aug. 96*	3.2/3.5[1]	Scar/fan survey/deposit map	2.7	Y	~25.0	4.8	10.8	60	Occurred after new lobe had filled up collapse scar of 28 and 31 Jul.
21 Aug. 96*	2.9/2.9[1]	Deposit map	2.2	N	~26.0	2.4	8.5		
2 Sep. 96*	~2.0	Scar/deposit estimate	1.5	N	~27.0	3.2	5.6	180	Occurred after new lobe had filled up collapse scar of 11 Aug.
3 Sep. 96*	~3.0	Scar/deposit estimate	2.3	Y	~26.0	3.2	8.8	240	Occurred after new lobe had filled up collapse scar of 11 Aug.
17 Sep. 96*	11.8/12.3[1]	Scar/Tar R survey	9.5	N	~27.0	2.3	35.2	480–540	Occurred after new lobe had filled up collapse scar of 2/3 Sep.
19 Dec. 96*	~4.0	No. flows/runout	3.1	Y	22.9	4.7	13.5	60	Related to new lobe on 12 Dec.
9 Jan. 97*	~2.0	No. flows/runout	1.5	Y	~31.0	11.1	4.8	70	Related to new lobe in SE overwhelming 17 Sep scar.
13 Jan. 97*	~2.0	No. flows/runout	1.5	Y	~34.0	9.9	4.4	140	
16 Jan. 97*	~3.0	No. flows/runout	2.3	Y	~34.0	9.3	6.8	60	Occurred after new lobe had filled up collapse scar of 9 Jan.
20 Jan. 97*	~3.0	No. flows/runout	2.3	Y	34.3	6.6	6.7	60	
30 Mar. 97	2.6[2]/2.6[1]	Estimate/survey Wht R	2.0	N	42.3	1.5	4.7	45	Occurred shortly after switch in dome growth, new lobe directed to S
31 Mar. 97	~1.0	Estimate Wht R	0.8	N	~40.0	1.3	2.0		Related to new lobe on 30 Mar.
11 Apr. 97	2.9[2]/3.0[1]	Estimate/survey Wht R	2.3	N	~43.0	3.4	5.3	180	Related to new lobe on 30 Mar.
25 Jun. 97	5.5[2]/6.4[1]	Survey Mosq/Trant/Belhm	4.9	Y	~68.0	6.4	7.2	25	Related to 17 May lobe overwhelming northern crater wall
3 Aug. 97	8.8[2]/9.1[1]	Estimate/survey Frt G	7.0	Y	~81.0	11.4	8.6	120–150	Occurred after switch in dome growth, new growth directed to W
21 Sep. 97	13.6[2]/14.3[1]	Survey Tuitts/ Wht G/Trant	11.0	N	61.6	2.8	17.9	20–30	Occurred shortly after switch in dome growth, new lobe directed to NE
4 Nov. 97	~2.0	Survey Wht R /Fan	1.5	N	64.1	3.4	2.3	45–70	Occurred shortly after switch in dome growth, new lobe directed to S
6 Nov. 97	~6.0	Survey Wht R /Fan	4.6	N	~65.0	12.9	7.1	35	Related to new lobe on 4 Nov.
26 Dec. 97*	55[3,4]	Scar estimate	46	Y	94.9	4.8	49.6	15–30	Related to lobe which filled up the collapse scar of 6 Nov.
3 Jul. 98*	20–25	Fan survey/scar estimate	15–19	—	~93.0	0	20.4	150	Occurred after cessation of lava extrusion
5 Nov. 98	~1.0[4]	Scar estimate	0.8	—	~77.0	0	1.0		Occurred after cessation of lava extrusion
12 Nov. 98*	~3.0[4]	Scar estimate	2.5	—	~76.0	0	3.3		Occurred after cessation of lava extrusion
20 Jul. 99*	~5.0[4]	Scar estimate	4.2	—	~64.0	0	6.6		Occurred after cessation of lava extrusion

* Dome collapses during which a significant portion of the flow entered the sea.
Valley abbreviations: Tar R, Tar River valley; Wht R, White River valley; Mosq, Mosquito Ghaut; Frt G, Fort Ghaut; Tuitts, Tuitt's Ghaut; Wht G, White's Ghaut; Trants, Trant's Yard and Belhm, Belham River valley. Deposit volumes represent non-DRE volumes, as measured in the field or estimated. Data include: (1) volumes of surge deposits calculated from mapped areas and estimated thickness. (2) Taken from Calder *et al.* (1999). (3) Total volume of dome rock (25×10^6 m^3) and talus (30×10^6 m^3) that entered the debris avalanche and pyroclastic density current, as estimated from the volume of the collapse scar. The volume of dome rock and talus involved in the pyroclastic density current alone is estimated as $35–45 \times 10^6$ m^3 by Sparks *et al.* (2002). (4) Scar volume rather than deposit volume. DRE values are calculated by assuming the dense rock has a density of 2600 kg m^{-3}, the pyroclastic flow deposits have a bulk density of 2000 kg m^{-3}, and the dome and scars have a bulk density of 2200 kg m^{-3}. The DRE collapse volumes are therefore calculated by multiplying the deposit volumes (including the surge component) by 0.77 and the scar volumes (indicated by (4)) by 0.84. Collapse volume is calculated using DRE collapse and DRE dome volumes. The data have been rounded to one decimal place. 'Hybrid swarms' indicates the occurrence of precursory hybrid earthquake swarms: Y, yes; N, no discrete earthquake swarms, although individual hybrid earthquakes may have occurred; –, no seismic activity. DRE dome volumes are based on dome surveys or, where written in italics, estimated by extrapolation of extrusion rate data. Extrusion rates are given as the 7-day running average (Sparks *et al.* 1998).

Velocity estimates for some pyroclastic flows have been determined by analyses of superelevation effects (Druitt *et al.* 2002*a*), seismic and energetic constraints (Sparks *et al.* 2002; Loughlin *et al.* 2002*a*, *b*) and video footage (Calder 1999). Average flow-front velocities were of the order of 3–10 m s^{-1} for small flows with runout <1 km, 5–20 m s^{-1} for medium flows with runout 1–3 km, and about 20–30 m s^{-1} for large to major dome-collapse flows, with runouts >3 km. Overriding pyroclastic surges varied from small, diffuse clouds to highly energetic pyroclastic surges that inundated large sectors of the volcano's flanks. Peak velocities of 70–90 m s^{-1} (Sparks *et al.* 2002) have been estimated for the 26 December 1997 energetic pyroclastic density current that devastated 10 km^2 of southern Montserrat. Velocity estimates and valley cross-sectional areas were used to calculate a peak flux rate of about 60 000 m^3 s^{-1} for the largest pyroclastic flow of the dome collapse of 25 June 1997. Quotient flux rates often exceeded valley retaining capacities, causing overspills to occur (Calder 1999; Loughlin *et al.* 2002*a*, *b*). Deposition and erosion by the flows themselves also modified topography and subsequently the flow path of following flows. Early pyroclastic flow deposition (e.g. during 25 June 1997 dome collapse; Loughlin *et al.* 2002*a*, *b*) reduced channel cross-sectional area, and enhanced the prospect of overspill of succeeding flows.

Seismicity and generation of pyroclastic flows

The seismic signals on Montserrat have been monitored by a maximum of 11 seismometers, including, since October 1996, an array of between one and five three-component broadband (0.03–30 Hz) instruments. Volcanic earthquakes have been categorized into the following earthquake types: volcanotectonic, hybrid, tremor and long-period (LP) earthquakes (Miller *et al.* 1998). Collapses of the lava dome (rockfalls to pyroclastic flows), explosions, crater-wall landslides and lahars also generated characteristic seismic signals (Miller *et al.* 1998).

Rockfalls and pyroclastic flows were associated with similar emergent, cigar-shaped waxing and waning seismic signals that had frequencies of 1–10 Hz and differed only in their durations and/or amplitudes (Fig. 3a, b). Source mechanisms and signal properties have been determined from broadband seismometers by Luckett *et al.* (2002). Two source mechanisms contributed to these seismic signals. (1) The flowing debris acted as a moving, rather inefficient surface source, generating a high-frequency (2–8 Hz) seismic wavefield. The amplitude of this high-frequency component depended on the magnitude of the event (i.e. the volume of the moving debris), but also on the relative positions of the seismometer and the flow. The signal at any station became stronger, then waned as the pyroclastic flow approached and subsequently moved past. Event durations were generally between 10 seconds and several minutes and were dependent on the runout distance of the rockfall or basal avalanche component of the flow. The large majority of these seismic signals were caused by small rockfalls that did not extend further than the edge of the dome talus, and which produced signals lasting for 40–120 seconds. (2) A long-period (LP) component (peak in spectral amplitude 1–2 Hz) occurred near the onset of most rockfall

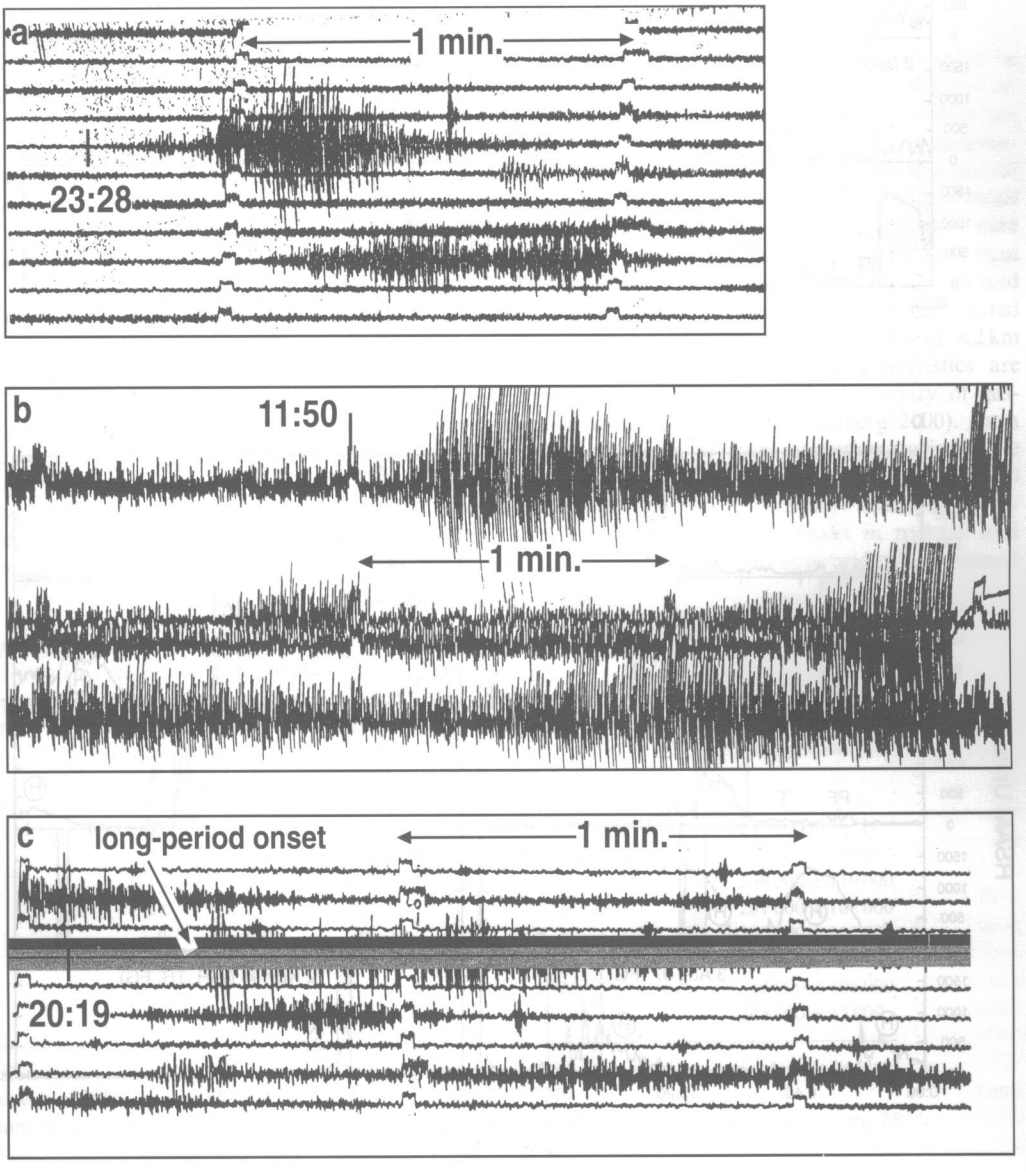

Fig. 3. Typical seismic signals associated with dome collapse. (**a**) Rockfall signal starting at 23:28 on 27 June 1996 from Gages (MGAT) short-period station. (**b**) Seismic signal of the onset of continuous pyroclastic flow activity in the Tar River valley, at 11:50 on 17 September 1996 from Gages (MGAT) short-period station. (**c**) Seismic signal of long-period/rockfall at 20:19 on 5 May 1997 from St Patrick's (MSPT) short-period station. This signal comprises a long-period signal immediately preceding the higher frequency rockfall signal. On each record the lines are ten minutes apart, and the tick marks are at one-minute intervals. All times are local (UTC – 4 hours).

signals (Fig. 3c). These consisted of an LP earthquake followed by a rockfall or pyroclastic flow within 10–20 seconds.

Most LP signals detected at Montserrat are interpreted as having a shallow source within the dome (Neuberg *et al.* 1998). Luckett *et al.* (2002) have shown that most dome rockfalls were preceded by, or contain, LP components throughout the signals. Synchronized field and seismic observations show that the initial LP component was sometimes associated with intense jets of gas and

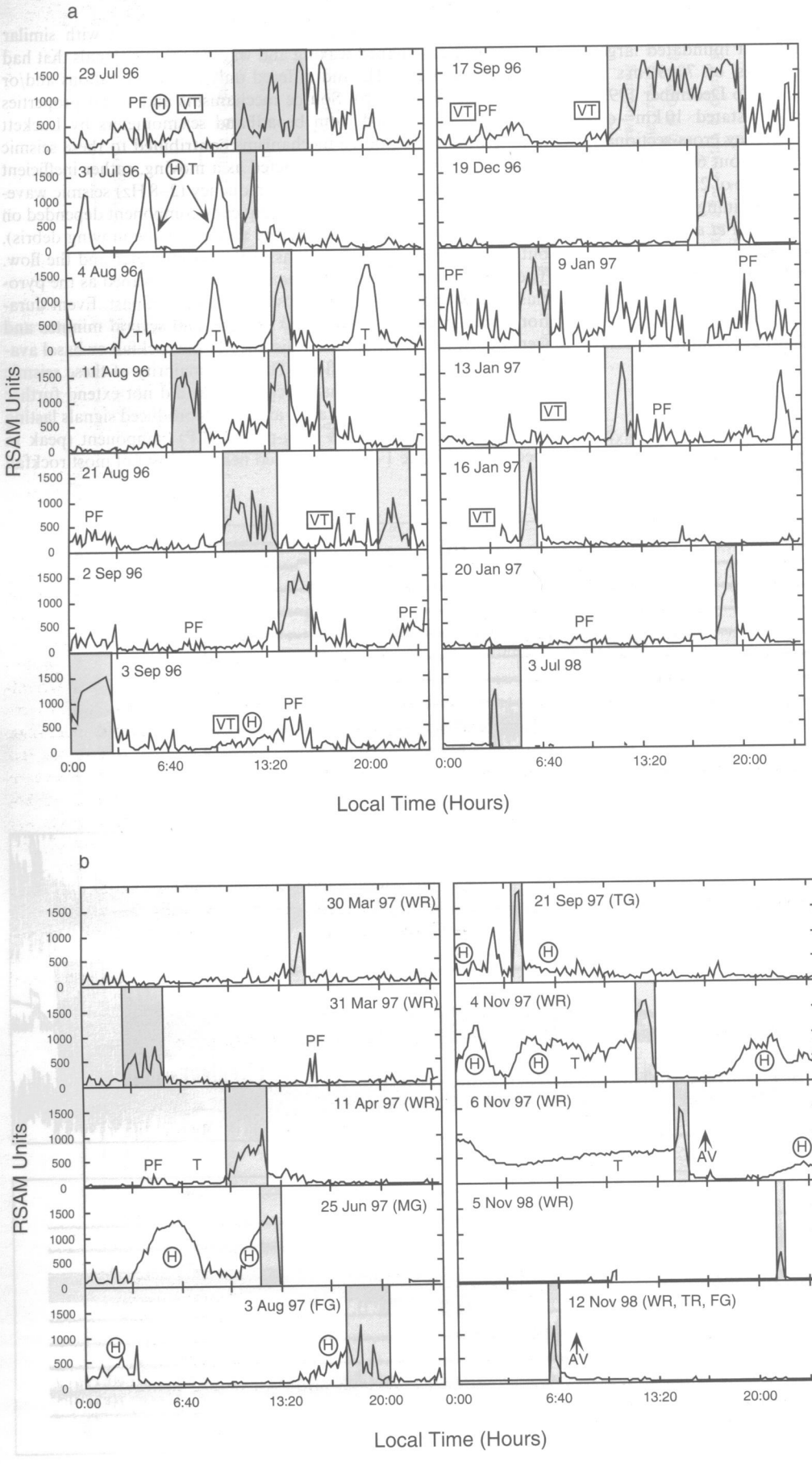

Fig. 4. (**a**) Ten-minute-average RSAM (real-time seismic amplitude measurement) plots of 14 large to major dome collapses down the Tar River valley for 24-hour periods. (**b**) Ten-minute-average RSAM plots of ten large to major dome collapses down the other valleys for 24-hour periods. Valleys are abbreviated as follows: WR, White River valley; MG, Mosquito Ghaut; FG, Fort Ghaut; TG, Tuitt's Ghaut; TR, Tar River valley. Shaded windows mark the main dome collapse periods. RSAM peaks generated by minor pyroclastic flow activity (PF), ash-venting (AV), hybrid (H), tremor (T) and volcanotectonic (VT) earthquake swarms are indicated. Several of the volcanotectonic earthquake swarms registered in 1996 were reclassified in 1997 as being hybrid earthquakes. RSAM has frequency-dependent clipping, so a limitation of this data is that clipping of high-amplitude signals is not easily observed graphically. All data were taken from Long Ground seismic station, just to the north of the Tar River valley (MLGT, Fig. 1), and the collapse events are listed in Table 1. Collapse events such as that of 3 August 1997 (9.1×10^6 m^3 non-DRE), which occurred on the western flank of the dome, register as less energetic than smaller events on the eastern side.

ash from the dome surface in the area where failure occurred. Observations of gas jets immediately preceding collapse have also been made at Mount Unzen Volcano (Sato *et al.* 1992; Ui *et al.* 1999). In contrast to these findings, Uhira *et al.* (1994) identified three phases in rockfall and pyroclastic flow signals at Mount Unzen. They observed wedge-shaped blocks of lava falling from a steep face and distinguished (1) block fall, (2) collision with the ground and (3) flow transport as essential components in exciting the seismic signals.

Yamamoto *et al.* (1993) and Uhira *et al.* (1994) reported that the volumes of pyroclastic flows shed from the Unzen dome (estimated by visual observation) were proportional to the maximum amplitude of seismic waves generated by the pyroclastic flow. Likewise, Norris (1994) used maximum seismic amplitude to investigate single-block failures at Mount St Helens. However, the area of broadband seismic amplitude envelopes is considered to be a more appropriate measure where pyroclastic flows occur continuously over a period of several hours (Norris 1994; Brodscholl *et al.* 2000). For Montserrat, broadband analyses of this type have not yet been undertaken. However, clearly the relationship between volume of pyroclastic flow and signal amplitude is not simple.

Here, we present seismic-energy data as measured by real-time seismic amplitude measurement (RSAM), which measures the average amplitude of seismic signals using a sampling rate of *c.* 60 per second (Endo & Murray 1991). Figure 4 illustrates 10-minute-average RSAM plots for 24-hour periods on the days of each of the large to major dome-collapse episodes from the Long Ground short-period seismometer (see Fig. 1). The collapses that descended the Tar River valley (Fig. 4a) are directly comparable as the flow paths are approximately constant, while those that travelled down the remaining drainages are shown in Figure 4b. Peaks in RSAM for the 29 July 1996 flows (deposit volume 3.0×10^6 m^3) are larger in amplitude than some volumetrically larger and wider-spreading flows later in the eruption (e.g. 3 July 1998, deposit volume 20–25 $\times 10^6$ m^3). Later flows travelled over a smooth surface of newly accumulated, unconsolidated deposits, which may have dampened the seismic signal. For a given collapse episode, correlation of seismic RSAM data with visual observations suggests that short, sharp RSAM peaks represented discrete pulses of large-volume, energetic flows.

Minute-scale pulses in collapse intensity are better identified using broadband seismic signals. Six main pulses ranging from 30 to 240 seconds in duration were identified from the 26 December 1997 collapse (Sparks *et al.* 2002, fig. 6). Three pulses, each less than 120 seconds in duration, were identified from the seismic signal of 25 June 1997 (Loughlin *et al.* 2002*b*, fig. 3). Moreover, these major pulses can be correlated with layers in the deposits (26 December 1997, Ritchie *et al.* 2002) and eyewitness accounts (25 June 1997; Loughlin *et al.* 2002*a*) respectively. Sequential flow pulses that occurred on these timescales are attributed to the retrogressive failure of individual portions of the dome.

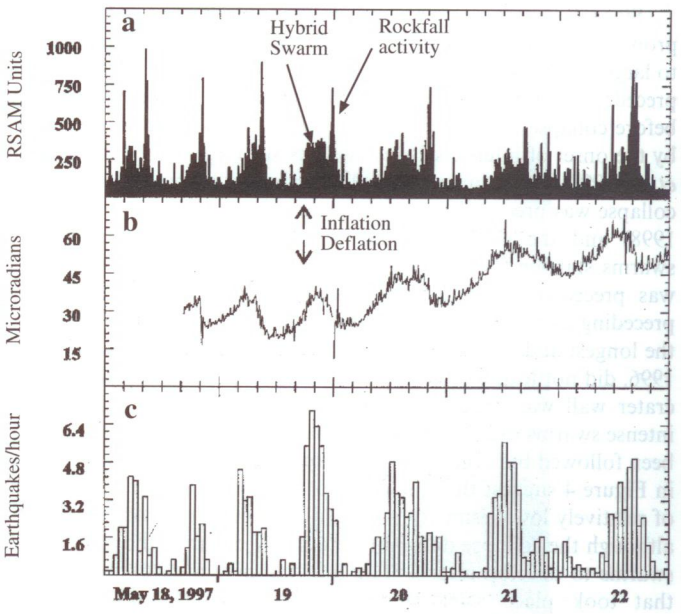

Fig. 5. Comparisons of (**a**) RSAM with (**b**) cyclic tilt records and (**c**) the total number of triggered earthquakes per hour for the period 18–22 May 1997. The triggered earthquakes are dominated by hybrid events that subsequently produce the cyclic, low-amplitude RSAM peaks. The large spikes in RSAM are rockfalls and small pyroclastic flows, produced at the onset of deflation. Spikes on tilt records represent noise (modified from Voight *et al.* 1998).

Most of the large dome collapses have been directly preceded by swarms of hybrid earthquakes (Table 1, Fig. 4a, b) (Miller *et al.* 1998; Voight *et al.* 1998). These swarms (more than ten events per hour) have been accompanied by cyclic crater-rim ground deformation (Voight *et al.* 1998, 1999). Hybrid earthquakes, the most prominent type of dome-related seismicity, have impulsive first arrivals and a long-period coda. Within swarms, hybrid earthquakes were often highly repetitive and occurred at regular intervals (less than a second to several tens of minutes), with similar waveforms and magnitudes (Miller *et al.* 1998). Hybrid earthquakes were located directly beneath the crater, at relatively shallow depths of <2 km (Aspinall *et al.* 1998), and their waveform characteristics are explained by interface waves generated at the boundary of gas-rich, bubbly magma embedded in a solid (Neuberg 2000). Lava extrusion appears to slow down or stop altogether during these shallow earthquake swarms. Swarms typically lasted for 3–30 hours, although on occasion swarms of a few days' duration occurred, notably in October–November 1996. Peaks in rockfall and pyroclastic flow activity generally occurred as hybrid activity waned (Fig. 5a).

Table 2. *Summary of pre-collapse cyclic eruptive activity as manifested by earthquake swarms, rockfall and pyroclastic flow activity, explosions and/or crater-rim deformation cycles*

Period	Cycle period (h)	Number cycles (before failure)	Peak tilt amplitude (μrad)	Extrusion rate (m s^{-1})	Extrusion/volume per cycle (m^3)*
Jul./Aug. 1996	4	>16	–	7–12	137 000 ± 36 000
Dec. 1996	6–8	8	1–2	4–6	130 000 ± 43 000
Jan. 1997	6–8	>15	1–2	6–12	238 000 ± 110 000
May 1997	12–18	>7	10–25	4–6	281 000 ± 108 000
Jun. 1997	8–12	9	30–40	5–8	245 000 ± 101 000
Jul./Aug. 1997	10–12	13	20–35	5–9	284 000 ± 104 000
Sep./Oct. 1997	9.7†	>75	–	6–12	314 000 ± 105 000
Dec. 1997	8–10	1	–	7–8	245 000 ± 43 000

*Time-averaged (7-day) extrusion rates (Table 1 and Sparks *et al.* 1998) for the periods listed are used to interpolate individual pulse volumes (volume/cycle = cycle period × extrusion rate).

†The intervals between explosions of September and October 1997 varied from 3 to 33 hours with an average of 9.5 hours for the 75 explosions (Druitt *et al.* 2002*b*).

Since July 1996, hybrid swarms have been characterized by a pronounced cyclicity (Table 2). The relationship of seismic swarms to large and major dome collapses is complex. Some collapses were preceded by one to several hybrid swarms in the hours and days before collapse (Fig. 4b). The 25 June 1997 collapse was preceded by the onset of intense seismic swarms starting on 22 June (Voight *et al.* 1998; Loughlin *et al.* 2002*b*). Similarly, the 3 August 1997 collapse was preceded by swarms starting on 31 July (Voight *et al.* 1998) and the 4–6 November 1997 collapse was preceded by swarms starting on 2 November. The 26 December 1997 collapse was preceded by an intense hybrid swarm that peaked in the preceding 24 hours (Sparks *et al.* 2002). On the other hand, one of the longest and most intense swarms, eight days in early December 1996, did not lead to a collapse although major deformation of the crater wall was produced. Indeed, there have been hundreds of intense swarms over the course of the eruption, and only a few have been followed by large collapses. However, the examples illustrated in Figure 4 suggest that the onset of intense swarms after a period of relatively low seismicity is indeed a precursor to large collapses, although the collapse does not necessarily occur in the *first* of such swarms to develop after a long quiescence. Large dome collapses that took place after lava extrusion had ceased present an exception, and were clearly not preceded by increases in seismic activity (Fig. 4a, b).

Particularly shallow or intense earthquake swarms can also trigger rockfalls by directly shaking the edifice. From December 1996 to March 1997, hybrid earthquakes shook the edifice and crater wall, clearly triggering both dome rockfalls and 'cold' landslides from the denuded area of the south crater (Galway's) wall. Although this generated many small rock avalanches, the maximum runout of these flows never exceeded *c.* 1 km. Moreover, the first large earthquake in any swarm produced the largest flows, dislodging the bulk of recently accumulated unstable material. Subsequent earthquakes in any swarm dislodged minor amounts of material, producing relatively small flows. Luckett *et al.* (2002) demonstrate that seismic signals generated by runout of the cold, crater-wall landslides are similar to the dome rockfall signals, but lack the long-period component. The generation mechanism of crater-wall landslides and some dome rockfalls may thus be attributed to seismic-shaking-induced instability. This mechanism is not, however, considered dominant with respect to most collapses of the growing dome. Indeed, during the cyclic patterns of ground deformation and hybrid seismicity described by Voight *et al.* (1999), dome collapses and rockfalls occurred predominantly in the deflation parts of tilt cycles, during declining seismicity.

Cyclicity and pyroclastic flow generation

A high-resolution tiltmeter was installed in December 1996 on Chance's Peak, *c.* 150 m from the crater rim (Voight *et al.* 1998, 1999). From January 1997 to August 1997, tiltmeter data displayed cyclic variations that correlated with seismicity and rockfall or pyroclastic flow activity (Table 2). The system was destroyed in mid-January 1997 but was re-established in May 1997 and operated until 5 August when the tiltmeter components were destroyed by Vulcanian explosions. The tiltmeters were high-gain, bubble-type biaxial-platform tiltmeters, with a resolution of 0.1 μrad. Digital time-series data were telemetered to the MVO at 8-minute intervals and analysed in near-real-time along with seismic RSAM data.

In December 1996, the tiltmeter revealed pressurization cycles with low-amplitude (1–2 μrad), inflation/deflation cycles superimposed on a steady, long-term drift. The cycle period was 6–8 hours and was clearly correlated with RSAM cycles. In May 1997, tiltmeters displayed a stronger rhythmic pattern of repetitive inflation–deflation cycles. Cycle amplitudes were in the range 10–25 μrad and each cycle lasted 12–18 hours, with the deflationary part of the cycle occurring more rapidly than the inflation (Fig. 5). Hybrid earthquakes occurred in increasing numbers as the inflationary part of the cycles progressed, sometimes merging into continuous tremor as inflation approached its maximum and then declined (Fig. 5). The peak in rockfall and pyroclastic flow activity occurred just after the onset of deflation during the waning hybrid swarm. The high peaks in RSAM are due to rockfalls and pyroclastic flows, and the lower-amplitude peaks are produced by the swarms of hybrid earthquakes. Tilt amplitudes declined after the end of May, but marked cyclic activity commenced again with an abrupt inflation at 05:30 local time on 22 June 1997, and was followed an hour later by a sharp deflation coincident with sustained pyroclastic flows down Tar River valley. This tilt excursion was the first in a series of nine, high-amplitude (*c.* 30 μrad), short-period (8–12 hour) cycles that culminated in the major dome collapse on 25 June 1997. The deflation that coincided with the collapse event was more pronounced than for the preceding cycles. By 10 July 1997, tilt amplitude had flattened and periods extended for 30 hours. High-amplitude cyclicity resumed on 31 July, and a major dome collapse occurred on 3 August. Vulcanian explosions started on 4 August 1997, and the tiltmeter was destroyed on 5 August (Druitt *et al.* 2002*b*). Since then, hybrid earthquake swarms have continued to serve as a proxy to define pressurization cycles.

The volume of magma extruded during each cycle has been estimated from time-averaged dome-extrusion rates and cycle periodicity (Table 2) and ranges from 140 000 to 320 000 m^3. For initial dome volumes (given in Table 1), each new cycle increased the dome volume by $0.4 \pm 0.2\%$. Assuming a simple geometry of an inflating half sphere, these volume increases correspond to cyclic inflation of only several tens of centimetres at the dome surface, as radius increases would have been 0.07–0.21%. Lava extrusion since April 1996 was, however, more characteristically marked by growth of discrete lobes along ductile shear zones in the upper portions of the dome (Watts *et al.* 2002). Active growth typically occurred either at the summit (Fig. 6a, b) or by advance of the steep headwall of a shear lobe (Fig. 6a, c). The headwalls of shear lobes had cross sections in the order of 10^4 m^2, so a cyclic pulse of dome extrusion of order $1–3 \times 10^5$ m^3 resulted in an advance of 10–30 m of the flow front in a few hours. Lobe headwalls were critically unstable, so a pulse-like advance inevitably resulted in elevated rockfall and pyroclastic flow activity. Lobe advancement rates, measured by theodolite, were about *c.* 30 m per day (on 6 March 1997) when the extrusion rate was 1–3 $m^3 s^{-1}$ and cyclic hybrid earthquake swarms were occurring.

Pyroclastic flow and rockfall activity occurring during the deflation stages of cycles normally comprised relatively small events, e.g. in May 1997 (Fig. 5). Large to major volume dome collapses occurred as the culmination of a period of between eight and 15 activity cycles, e.g. December 1996; January and June 1997. Major dome collapses, which occurred during magma extrusion, followed dome volume increases of $1–5 \times 10^6$ m^3 over timescales of a few days. There are, however, some exceptions, e.g. the major 26 December 1997 collapse event occurred at the end of the first and only cycle in that period (although it was 37 hours long). During the August 1997 explosive period, Vulcanian explosions occurred at the end of each individual earthquake and tilt cycle (Druitt *et al.* 2002*b*). The period of the September/October 1997 explosions was marked by little evidence for cyclicity other than the explosions themselves. Hybrid earthquake swarms were absent and tilt data were unavailable.

Magma extrusion and dome size in relation to pyroclastic flow generation

The rate of magma extrusion and dome growth has had a primary effect on eruptive style and has played a fundamental role in hazards assessment throughout the eruption (Sparks *et al.* 1998). For the first 11 weeks following the onset of dome extrusion in November 1995, lava extrusion rates were low (*c.* 0.5 $m^3 s^{-1}$). After February 1996, extrusion rates increased to 2.1 $m^3 s^{-1}$ (Fig. 7a) (Sparks *et al.* 1998). A further, marked increase occurred at the end of May 1997, with extrusion rates ranging from 4 to 13 $m^3 s^{-1}$, with substantial fluctuations to December 1997. The tendency during the November 1995–March 1998 period has been for extrusion rate to increase with time (Sparks *et al.* 1998), although this is

(a)

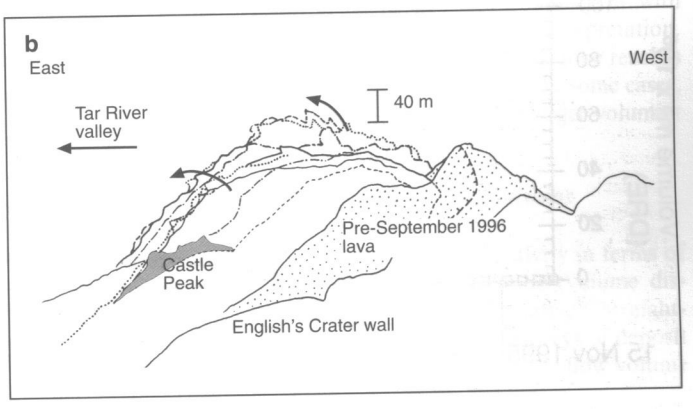

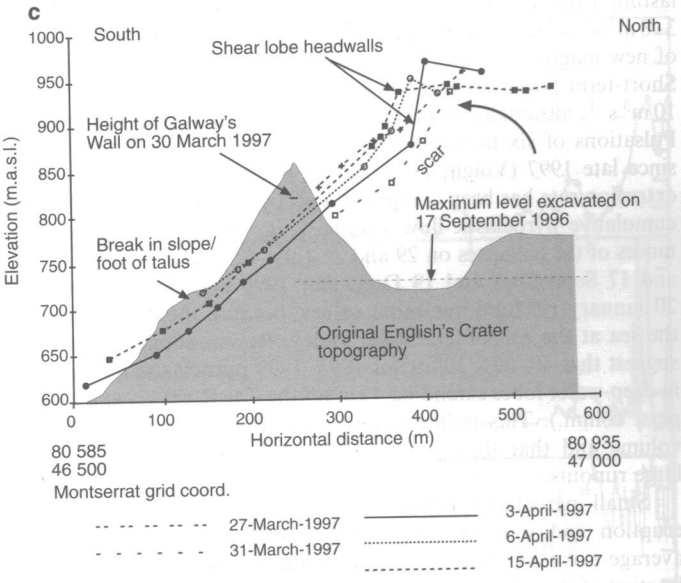

Fig. 6. (**a**) A shear lobe on 15 April 1997, moving southwards towards the White River valley. The steep platey upper surface is a slickensided ductile shear zone of highly crystalline lava, with the headwall represented by the ragged surface of jointed lava (left). The shear zone within the dome controls the geometry of the extruded shear lobe, with the rate of shear lobe advance controlled by magma extrusion rate. Most pyroclastic flows originate from instability of the headwall, and the slight concavity of the surface shown is a collapse scar. Collapse of the headwall led to numerous pyroclastic flows in this sector during April–May 1997. Topographic profiles through the headwall are shown in (c). (**b**) Nine dome growth profiles determined photographically from a position 3 km north of the dome (Fig. 1, Harris Lookout) for the period 1 December 1996 to 27 March 1997. This period shows regrowth of the dome after the 17 September 1996 explosive activity. Summit growth occurred by the sequential extrusion of spines and vertically to southeasterly directed shear lobes (25 December 1996 and 21 January 1997 lobe; Watts *et al.* 2002). (**c**) N–S profiles through the southern wall of English's Crater (Galway's Wall) and growth of the 27 March and 13 April 1997 lobes taken from global positioning system/laser binocular data. The original topography of English's Crater is shaded (note that Galway's Wall deteriorated significantly during this period allowing rockfalls to be shed into the White River valley by 30 March) and the maximum level of excavation of the explosive activity of 17 September 1996 is indicated. Collapses occurred on 30 March and 11 April 1997 with subsequent growth occurring in the scar of the previous collapse. The headwalls of these southerly directed shear lobes represented large unstable masses perched above the Galway's Soufrière area.

considered unusual in other dome-forming eruptions (Nakada *et al.* 1999). Extrusion rates for the Soufrière Hills dome (1–13 $m^3 s^{-1}$) are, however, similar to those of many other dome-forming eruptions as reported by Newhall & Melson (1983). The *c.* 0.3 km^3 of andesite erupted by March 1998 was partitioned into: 113×10^6 m^3 (DRE) volume of the dome on 10 March 1998 when its growth ceased; 150×10^6 m^3 volume of accumulated pyroclastic flow deposits; and 28×10^6 m^3 of explosive ejecta.

Extrusion-rate pulses have occurred on timescales ranging from a few hours to months (Fig. 7a). Three long-term pulses

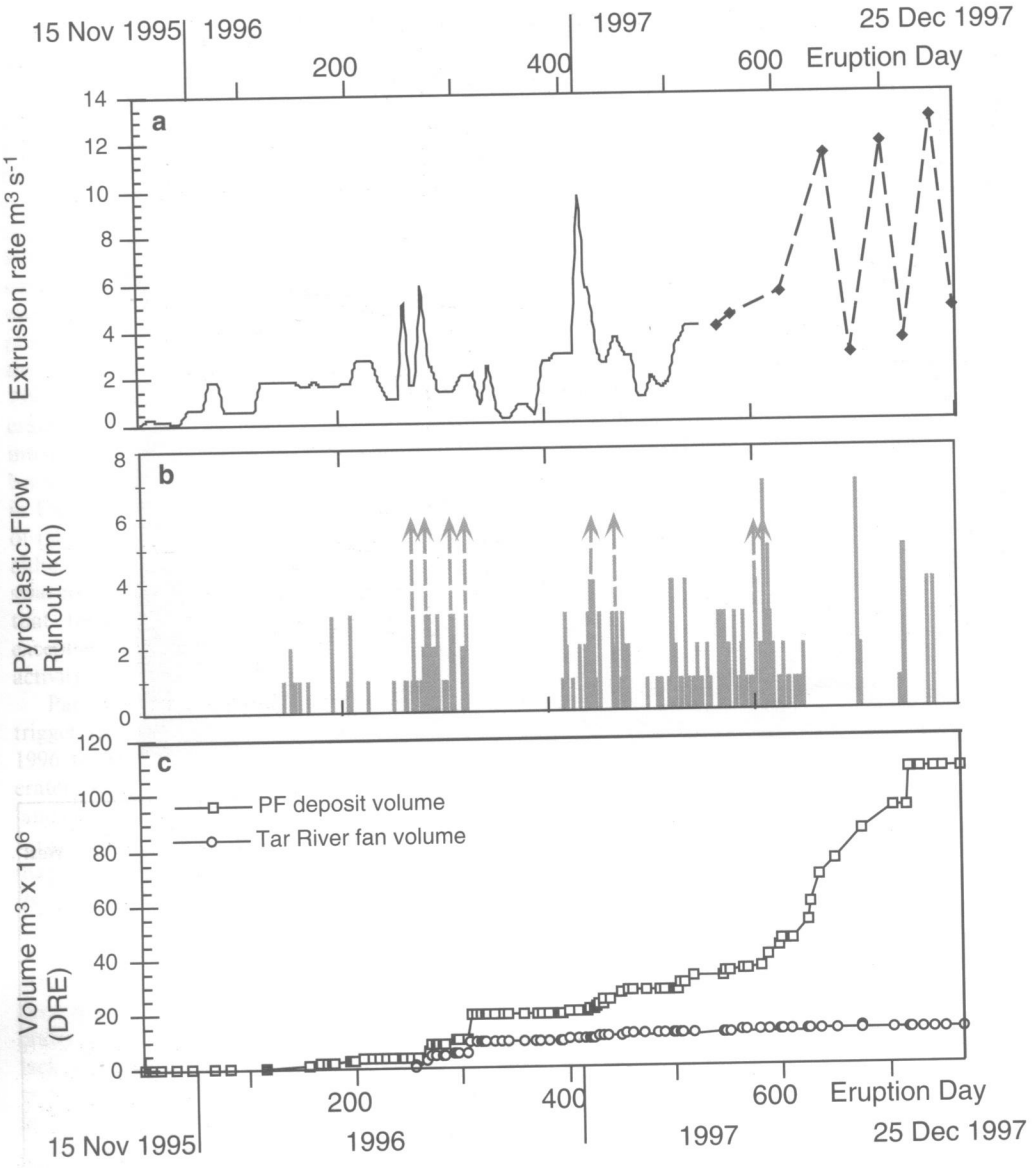

Fig. 7. Dome growth in relation to pyroclastic flow runout and deposit volumes. (**a**) Weekly running-average dome-extrusion rate (dashed line is shown where volume estimates are spaced at more than one month intervals). (**b**) Runout distances of pyroclastic flows. The runouts of major collapses that entered the sea have been approximated (dashed arrows). (**c**) Cumulative pyroclastic flow deposit volume. Modified from Cole *et al.* (1998).

lasting a few months have been identified with extrusion rates of 3–8 $m^3 s^{-1}$. These pulses reflect processes at depth, such as influxes of new magma into an open-system chamber (Sparks *et al.* 1998). Short-term pulses lasting a few days reach extrusion rates of over 10 $m^3 s^{-1}$, although 5–8 $m^3 s^{-1}$ represents a more realistic average. Pulsations of six to seven week cycles have been well established since late 1997 (Voight *et al.* 1999). The weekly running-average extrusion rate has been compared with pyroclastic flow runout and cumulative pyroclastic-flow volume (Fig. 7b, c). The runout distances of the collapses on 29 and 31 July, 4, 11 and 21 August, 2, 3 and 17 September and 19 December 1996 and on 9, 13, 16 and 20 January 1997 are minimum values, because these flows entered the sea at the end of Tar River valley. Recent submarine surveys suggest that 40–60 $\times 10^6$ m^3 of 1995–1999 pyroclastic material lies in deep-water lobes extending 4 km off the Tar River coast (S. Carey pers. comm.). This indicates that these flows were substantial in volume and that they and their derivative submarine flows had large runouts.

Small pyroclastic flows occurred frequently throughout the eruption and were typically associated with periods of low to average extrusion rates (1–3 $m^3 s^{-1}$), but account for only a small fraction of the total volume erupted. Large to major dome collapses were preceded and followed by periods of elevated extrusion rate (4–8 $m^3 s^{-1}$), (e.g. 29–31 July, 11 August 1996). In particular, the periods of late July and December 1996 were characterized by a closely spaced series of large dome collapses, which continued for a month. Dome growth was focused in localized areas by easterly directed shear lobes. These lobes rapidly produced oversteepened, unstable flanks and generated relatively large collapses. Each collapse scar was infilled quickly with several million cubic metres of new lava within a few days, and the failure cycle was then repeated. A few periods may have reached less substantial extrusion rates. Only moderate extrusion rates (*c.* 2.1 $m^3 s^{-1}$) appear to have preceded the 17 September 1996 explosive eruption, although data during this period are not well constrained. Likewise, the March–April 1997 collapses occurred in association with magma discharge rates of 1–3 $m^3 s^{-1}$. These collapses were associated with the development of a particularly unstable shear lobe over Galway's Wall (Fig. 6b), and were preceded by increased numbers of long-period earthquakes, suggesting increased gas and pressure build-up within the dome.

The capacity for generating large-volume collapses clearly depends on the dome volume. Estimated collapse volumes have been normalized to respective initial dome volumes in Table 1 and Figure 8. Most large (1–4 $\times 10^6$ m^3) and major (>4 $\times 10^6$ m^3) collapses represented <18 vol% of the dome with no systematic change (in actual collapse volume or percentage collapse volume) over eruption duration (Fig. 8a, b). Clearly, however, as dome volume increases, a collapse of *c.* 18 vol% will mean successively larger volume collapses. The explosive eruption of 17 September 1996, the debris avalanche and dome collapse of 26 December 1997 and the collapse of 3 July 1998 (post-extrusion collapse) were clear exceptions, representing outliers in the data with collapses of *c.* 35, *c.* 50 and 20 vol% respectively (Fig. 8c; Table 1). In general, volume percentage collapse is therefore independent of dome volume (Fig. 8c) and average extrusion rate (Fig. 8d) for these ranges.

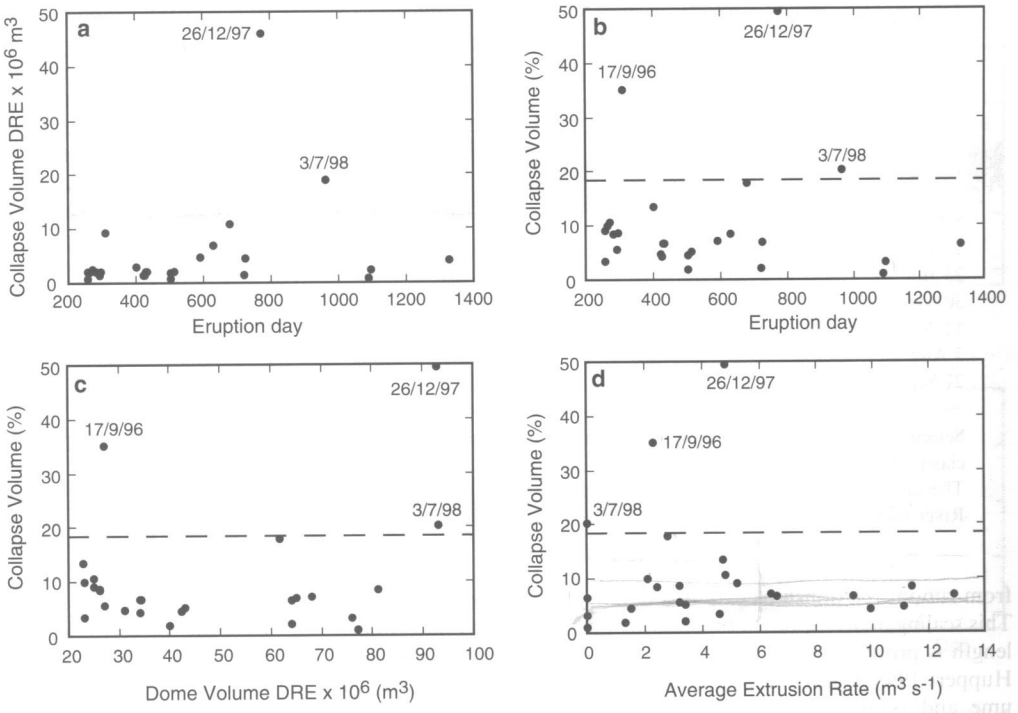

Fig. 8. (**a**) Measured collapse volume (DRE $\times 10^6$ m^3) against time (eruption day) for the 25 dome-collapse events in Table 1. (**b**) Percentage collapse volume (calculated using collapse volumes and initial dome volumes from Table 1) against time. Percentage collapse volume plotted against (**c**) dome volume and (**d**) seven-day running average lava extrusion rate. The zone under the dashed line in (b–d) marks percentage collapse volumes of <18 vol%, within which most dome collapses lie.

For periods of up to several weeks, low cloud cover over Soufrière Hills obscured direct visual observations of the dome. Rockfall activity, as interpreted from seismic data, has thus been used as the principal indicator of the status of the volcano. There have been several periods, however, when rapid dome growth occurred without accompanying seismic activity (Sparks *et al.* 1998; Miller *et al.* 1998). Daily rockfall counts from the seismic records over a three-month period from 1 May to 1 August 1996 (Fig. 9) show marked fluctuations over a relatively short period, and a decline in rockfall frequency in July 1996. During the same period, however, rockfall amplitudes steadily increased. Dome volume estimates suggest that during that time the magma extrusion rate was increasing markedly (from *c.* 2 to *c.* 6 m^3 s^{-1}). The relationship between rockfall activity and extrusion rate is therefore complex and rockfall counts need to be considered in conjunction with rockfall amplitude and duration data for meaningful interpretation. Local topography can also be important: when a shear lobe reaches a steep slope, rockfall activity is enhanced although, in some cases, rockfalls may occur less frequently while involving larger volumes.

Pyroclastic flow magnitude–frequency relationships

It is instructive to characterize pyroclastic flow activity in terms of frequency (in number of events) versus magnitude (volume dislodged). For larger-scale dome collapses this is relatively straightforward and achieved by event recording and by surveys of deposit volumes. An indirect method of estimating pyroclastic flow volume

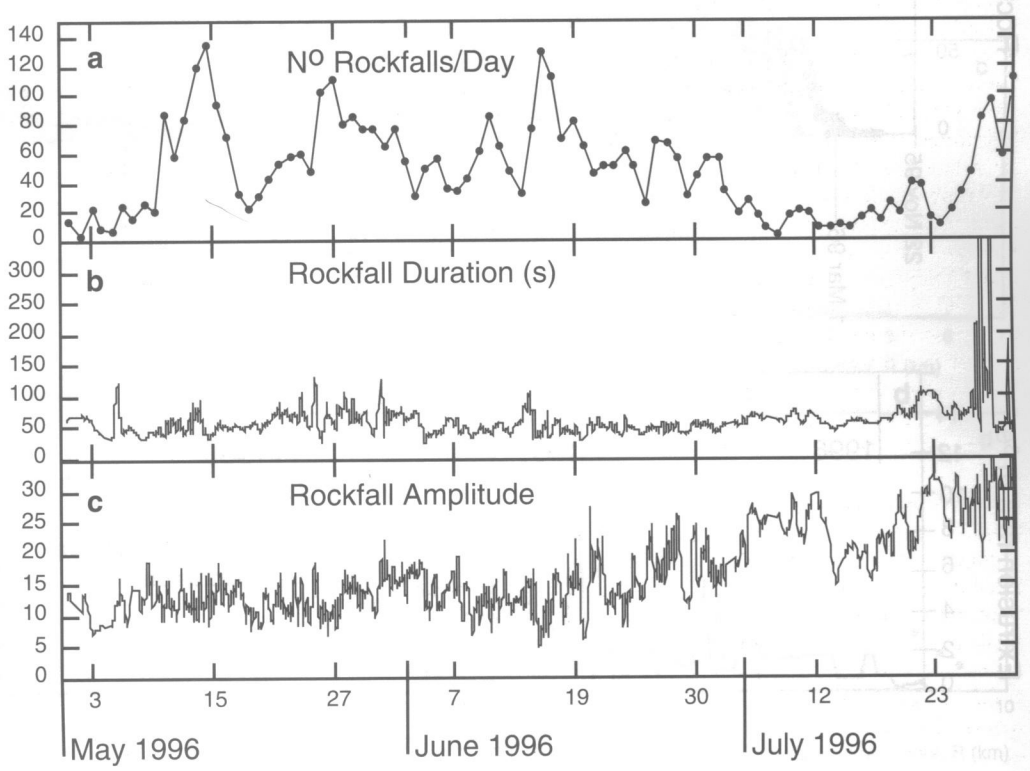

Fig. 9. The number of rockfalls per day over the period 10 May–1 August 1996. Rockfall duration data are largely constant, with a sharp increase at the end of July when many small pyroclastic flows were produced. The data show increasing rockfall amplitudes since late June, even though rockfall activity (as measured by event frequency) appears to have been low from late June to late July. Data shown in (b) and (c) are running averages of the raw data.

Table 3. *Flow runout for selected medium to major dome collapses*

Date	Runout (km)	Volume ($\times 10^6$ m^3)
3 Apr. 96	1.6	0.15
12 May 95	2.9	0.33
31 Mar. 97	2.5	0.16
5 Jun. 97	3.1	0.38
17 Jun. 97	3.9	0.77
25 Jun. 97	6.7	5.5
30 Mar. 97	3.6	2.6
11 Apr. 97	4.1	2.9
3 Aug. 97	5.6	8.8
21 Sep. 97	6.0	13.6

Selected from Calder *et al.* 1999. Volumes of deposits of pyroclastic flows (non-DRE), excluding surge components (Table 1). The runout for 31 March 1997 is for flows shed down in the Tar River valley in the afternoon of that day.

from runout relationships can also be utilized (Calder *et al.* 1999). This scaling analysis, based on empirical data, suggests that runout length is proportional to volume to the one-third power (Dade & Huppert 1998; Calder *et al.* 1999). Selected, well constrained, volume and runout data for Montserrat dome collapse flows are summarized in Table 3 (and illustrated in Calder *et al.* 1999, fig. 2).

For rockfalls and small pyroclastic flows, the frequency–magnitude relationship is more accurately investigated using seismic data. Relative event magnitudes can be determined using parameters such as signal duration and/or amplitude. Automatic triggering by seismic software ensures that even small events are accurately counted and that records are complete for night-time events, as well as for those when observation conditions are poor.

Between 3 January 1996 and 1 December 1998, 27 150 rockfalls triggered the short-period seismic network. During triggering, magnitudes of events were not differentiated, so that larger pyroclastic flows were also incorporated. Their numbers are comparatively small, however, and do not significantly influence the trend. Rockfalls and pyroclastic flows with runouts of less than 1 km were commonly generated 20–150 times a day (Fig. 10), although during certain periods of the eruption rockfalls were almost absent. Low rockfall counts (<20 per day) were characteristic of periods when extrusion rate was either low or zero (before March 1996 and March–July 1998), or when the dome was small and the rockfalls produced were too small to trigger the seismic network (pre-1996 and 17 September–December 1996).

For the period November 1995–September 1997, the maximum amplitude and duration of rockfall and pyroclastic flow signals were measured by MVO staff manually from the paper records of the short-period seismometers. Maximum-amplitude data were frequently clipped (true maximum not recorded) but rockfall and pyroclastic flow durations exhibited variations that could clearly be correlated to observed volcanic activity. The first three and a half

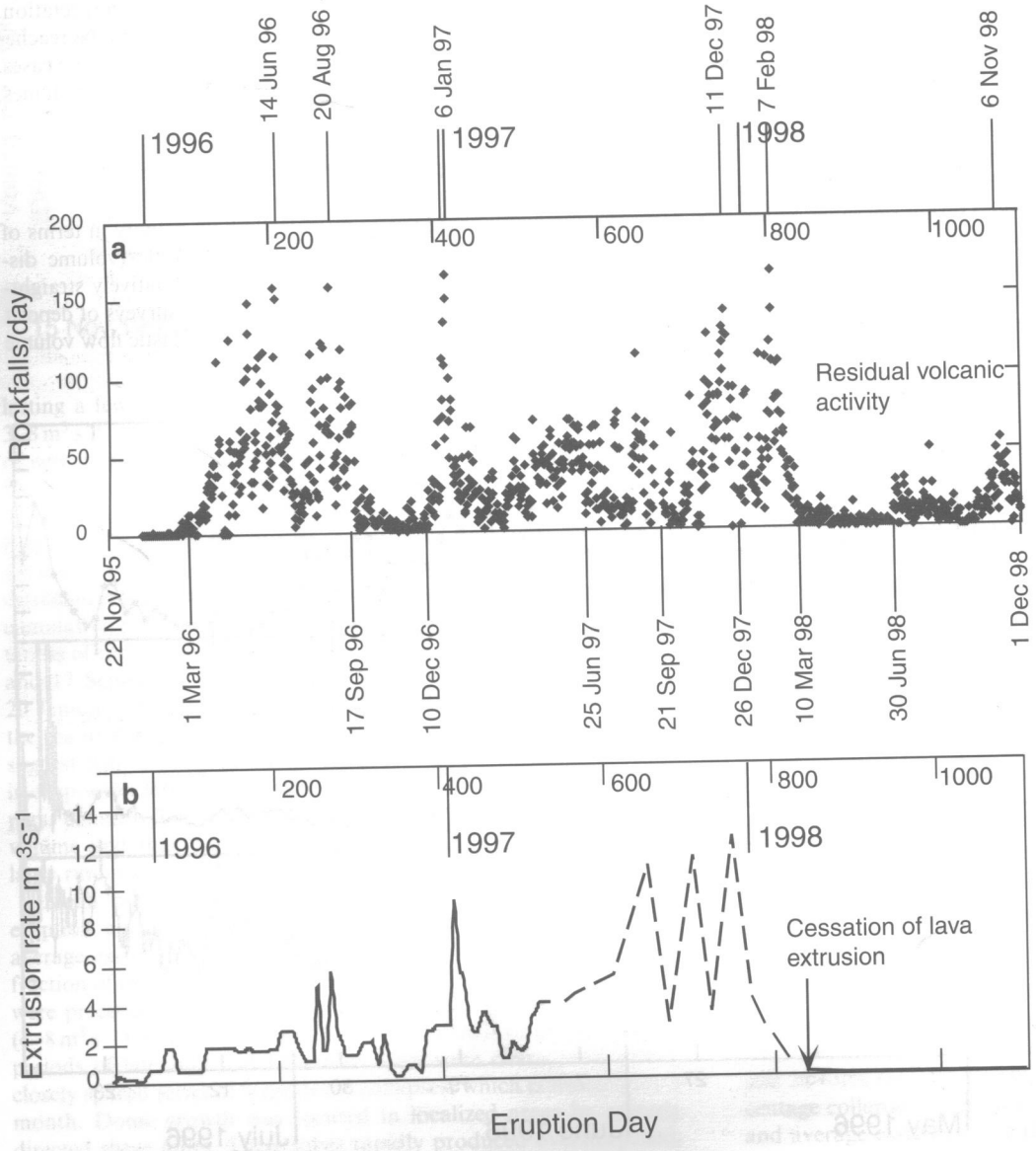

Fig. 10. (**a**) Number of rockfalls per day throughout the eruption, as counted by triggering of the broadband seismic network. Dates for the peak numbers are labelled above the figure, and the troughs below. Periods when rockfall frequency is low are 22 November–1 March 1996 (extrusion rate 0.5–2 m^3 s^{-1}), after the 17 September 1996 explosive activity (dome growth did not recommence again until 1 October and significant rockfall activity recommenced around 10 December), during the 22 September–21 October 1997 Vulcanian explosions, and after lava extrusion ceased (10 March 1998) until 30 June 1998. Periods characterized by elevated rockfall activity have occurred prior to large collapse events (e.g. 6–12 January and 11–26 December 1996). The major collapses of 25 June and 21 September 1997 were not preceded by rockfall spikes. The collapses of 28 July 1996 and 26 December 1997 occurred immediately after periods of anomalously low rockfall activity. (**b**) Weekly running-average extrusion rate for the same period.

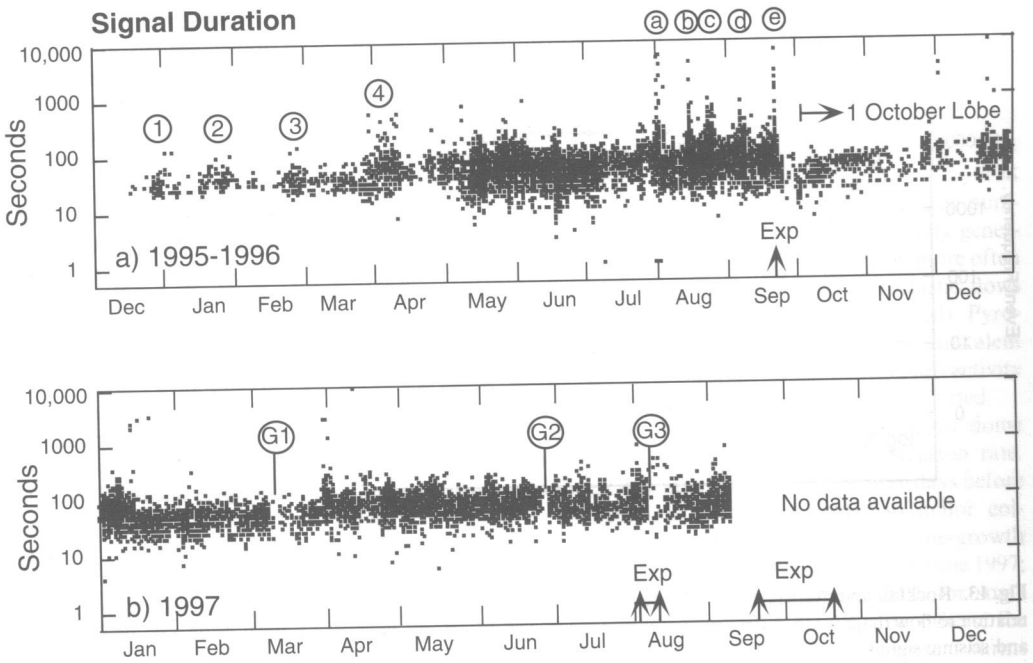

Fig. 11. Rockfall durations in seconds for the period December 1995 to September 1997, as measured manually from the seismic paper records by MVO staff. Pulses in rockfall activity are labelled 1–4 and a–e, and gaps are labelled G1–G3. The periods of explosive activity of 17 September 1996 and August and September–October 1997 are also indicated.

months of dome extrusion were characterized by relatively few, short-lived rockfalls occurring in four discernible pulses, each of two to four weeks' duration (Fig. 11a, 1–4). On around 16 April 1996, the rockfall record became more continuous, with significant numbers of rockfalls beginning to exceed 100 seconds in duration. These represent the first rockfalls and pyroclastic flows out of English's Crater, and they coincided with the development of the first shear lobe of the lava dome (25 April 1996 lobe), which by the end of April had advanced over the steep front of the 350-year-old Castle Peak Dome (Watts *et al.* 2002). An abrupt increase in rockfall activity occurred on around 8 May 1996 and four days later the first pyroclastic flows reached the sea 2.7 km from the dome. Between the end of July and mid-September 1996, five distinctive peaks in activity occurred spaced at one to two week intervals (Fig. 11a–e). This phase culminated in the 17 September 1996 sub-Plinian explosive activity. Subsequent growth of the 1 October lobe was characterized by sparse rockfalls until around 15 December 1996. The remaining period, January to September 1997, was characterized by relatively high activity with subtle pulsations in rockfall numbers and durations. During this later period, conspicuous gaps in the data exist for around 10 March, 24 June and 3 August 1997 (G1, G2, G3 respectively in Fig. 11b). A frequency histogram of rockfall and pyroclastic flow durations has been compiled from these data for the 22-month period December 1995 to September 1997, and the plot suggests an approximately normal distribution (Fig. 12a). For a subset of rockfalls and pyroclastic flows ranging in duration between 60 and 500 seconds (considered more realistic values), a linear relationship is generated on a log–log plot (Fig. 12b).

Pyroclastic flow runout distance data were compiled from a number of sources (Fig. 12c). Commonly, runouts of observed medium to large flows were recorded in the MVO observations book and broadcast in daily reports. Flows that occurred at night were only observed seismically, so that runouts were ascertained by inspection of the deposits the following day. For small to medium flows, reported observations were augmented by information from

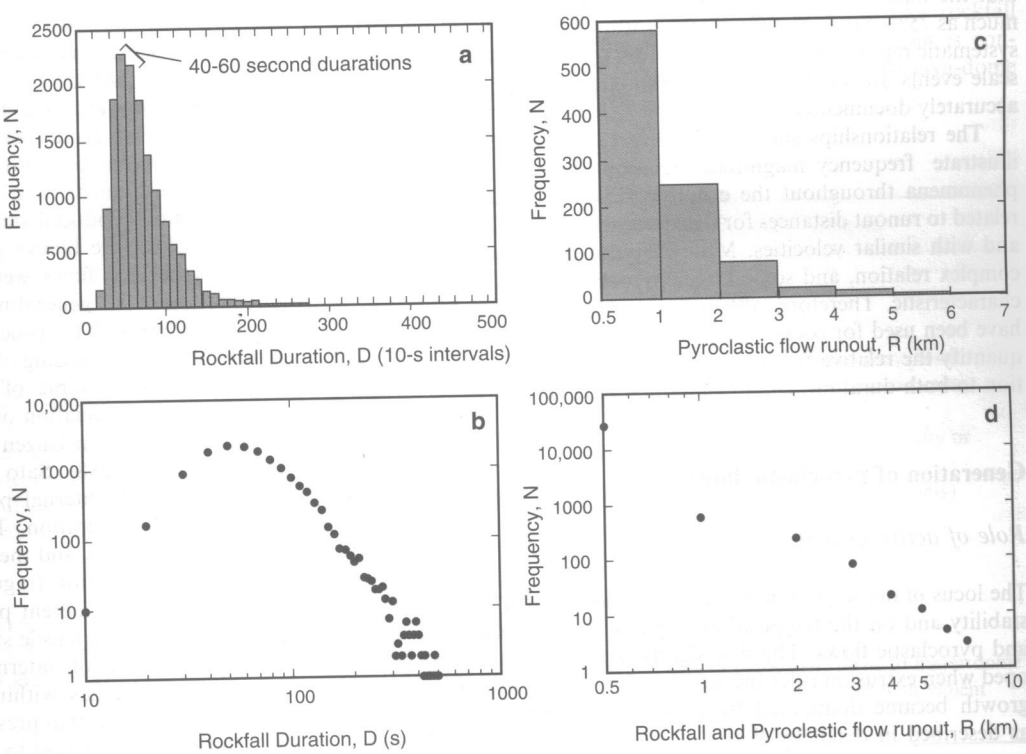

Fig. 12. (**a**) Frequency histogram of rockfall duration data for the period December 1995 to September 1997 (Fig. 11). Durations are categorized in 10-second intervals. (**b**) Log plot for the rockfall duration (20–500 seconds) frequency data. (**c**) Frequency histogram of pyroclastic flow runout distances throughout the eruption. Runouts have been estimated to the nearest kilometre and are categorized in 1-km bins. (**d**) Log plot for the pyroclastic flow runout–frequency data. These data include the number of rockfalls taken from the seismic broadband triggers. All rockfalls are assumed to have runouts of <500 m.

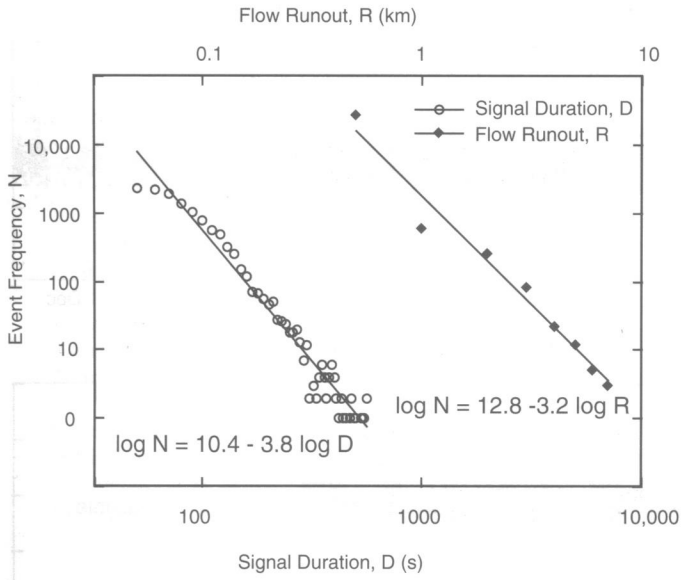

Fig. 13. Rockfall and pyroclastic flow frequency (in number of events, N) in relation to flow magnitude as determined by runout, R, for pyroclastic flows and seismic signal duration, D, for rockfalls.

the seismic paper records, which provided an accurate account of the number of events where 'several' or 'continuous small scale pyroclastic flow activity' was otherwise recorded. We also used the assumption that where 'several' flows were reported, five occurred and that flows recorded as being in the 'upper Tar River valley' had runouts of between 0.5 and 1 km. Figure 12d includes rockfalls as obtained from seismic-trigger event counts. Low-amplitude rockfall signals with durations of <3 minutes have been correlated visually with rockfalls travelling <0.5 km. Thus, the majority of these signals (*c.* 27 100) can be reasonably attributed to the <0.5 km category. The results suggest a linear relationship between frequency and runout between 0.5 and 7 km on the log–log plot. Vertical error bars for rockfall numbers are smaller than the scale of the symbol, as these were counted automatically by seismic software. The data show that moderate events (1–3 km runout) occurred, on average, *c.* 15 times a month, while large dome collapses occurred on average once every one to two months. The plot also suggests, as to some extent anticipated by recording bias, that the number of 0.5–1 km flows may be underestimated by as much as 75%. Small pyroclastic flows were frequent enough to defy systematic reporting. Vertical-axis errors for the moderate- to large-scale events are small, as these events are less numerous and are accurately documented.

The relationships shown in Figure 12b and d can be used to illustrate frequency–magnitude relationships of dome-collapse phenomena throughout the eruption. Event durations should be related to runout distances for collapses generated as discrete pulses and with similar velocities. Multiple-pulse collapses have a more complex relation, and some larger pyroclastic flows exhibited this characteristic. Therefore, although different graphical approaches have been used for rockfalls and larger pyroclastic flows, the data quantify the relative frequencies of various sizes of events in relation to both duration, D and runout, R (Fig. 13).

Generation of pyroclastic flows

Role of active growth areas

The locus of dome growth has been a major control on both dome stability and on the temporal and spatial distribution of rockfalls and pyroclastic flows. The first significant pyroclastic flows developed when extrusion rates increased to 2 $m^3 s^{-1}$ or more, and dome growth became dominated by exogenous 'shear lobe' extrusion, as described in detail by Watts *et al.* (2002). Lava was extruded asymmetrically from the central vent and broke out through the old dome carapace to form a lobe with a blocky, steep headwall from which rockfalls and pyroclastic flows were generated (Fig. 6a, b, c). The steep headwall often developed where the lobe met a steep slope. In this case, the front stagnated and further advance was accommodated by avalanches and rockfalls. The flow front could thus stay relatively stationary for periods of days to weeks, although it was continually fed by flow of lava behind. The area below the headwall commonly became incised by deep erosion chutes due to repeated passage of rockfalls.

A major feature of dome-growth evolution at Montserrat was the sudden switching of extrusion direction. A given lobe would be active for many weeks and then stagnate, and a new lobe would develop in a different direction. In many cases, large to major collapses and pyroclastic flows were associated with a switch in active area and establishment of a new lobe (Table 1). New lobes were often extruded within the scar of a previous collapse, and substantial new collapses occurred once the scar had refilled. Large collapses of older parts of the dome commonly occurred during switches in extrusion direction due to push-up of older lava by the incipient formation of a new lobe below (e.g. 4 November 1997, Table 1). The generation of pyroclastic flows with runouts >1 km was commonly associated with collapses of fresh lava and newly extruded parts of the dome, and was therefore intimately linked with shear-lobe extrusion.

The fragmentation of vesicular crystal-rich andesite

The Soufrière Hills magma is a crystal-rich andesite (58.5–60.6 wt% SiO_2), which has shown no significant variation in bulk chemistry since the beginning of the eruption (Murphy *et al.* 1998, 2000). The phenocryst assemblage of the dome lava consists of plagioclase (28–30 vol%), amphibole (3–10 vol%), orthopyroxene (2–5 vol%) and oxides. The total crystal content of the rapidly erupted lava is 65–75 vol% with 35–50 vol% phenocrysts and 20–25 vol% groundmass microlites (<80 μm). The remaining 25–35 wt% magma comprises high-SiO_2 rhyolite glass (76–80 wt% SiO_2), partly devitrified (Murphy *et al.* 1998). In slowly erupted lava, the glass content can reach as low as 5–15 vol% due to additional microlite crystallization in the conduit. The initial melt phase of the source magma contains 4–5% water at 5–6 km depth with a bulk magma water content of about 1.6 wt% (Barclay *et al.* 1998; Murphy *et al.* 2000). Magma rheological properties vary from a crystal-rich magma (25–35 vol% rhyolitic melt with 4–5 wt% H_2O) with viscosity 10^6 Pa s to a degassed crystalline lava (5–15 vol% melt) with an apparent viscosity as much as 10^{14} Pa s and considerable strength (Sparks *et al.* 2000).

Spontaneous autobrecciation of incandescent blocks of lava was observed during dome rockfalls and pyroclastic flows, especially at night (e.g. December 1996). Large blocks fragmented during initial stages of movement, and after impact with the ground surface disintegration produced small, fines-rich pyroclastic flows. On two occasions, discrete blocks projected from the basal flow front of small pyroclastic flows were seen to exfoliate rapidly (from the outside inwards), generating a trailing plume of ash behind the projecting block. This process may also help to explain the commonly observed rounding of relatively dense juvenile blocks, which occurred even in some of the smallest-volume pyroclastic flow deposits. Autobrecciation of hot microvesicular lava has also been recognized at Mount Unzen (Sato *et al.* 1992) and Mount St Helens (Mellors *et al.* 1988). Sato *et al.* (1992) postulated that the lava blocks had high internal pore pressure and low tensile stresses, facilitating disintegration. They considered the landing shock of blocks on the slope, and the shearing at the base of the flow, to be the main triggers for fragmentation. Autobrecciation has been interpreted as an inherent property of these lavas above a critical temperature (where tensile strength is relatively low).

The influence of internal pore pressure is also of critical importance. The gas within hot dome rock with a porosity of 10 vol% and an internal pressure of 1 MPa will expand to ten times its volume when released to atmospheric pressures during collapse

(Sparks 1997). The actual gas pressure in the Montserrat dome may have greatly exceeded this pressure (Voight & Elsworth 2000). Pressurized gas can be trapped in vesicles (which can burst when confining pressure is removed) and can also occur in pressurized volatiles diffusing through crack-permeable magmas (Voight & Elsworth 2000). This gas-expansion mechanism is a major factor in the generation of energetic pyroclastic currents associated with the large Montserrat dome-collapse pyroclastic flows (Woods *et al.* 2002). Observations suggest that, in most pyroclastic flows, the process of fragmentation and pyroclastic surge generation is highly dynamic and continues to occur during disintegration of blocks in the moving pyroclastic flow, as well as at the collapse onset.

Discussion

The question 'did it fall or was it pushed?' is one that has preoccupied workers concerned with the generation of dome-collapse pyroclastic flows. It appears that both of these scenarios can, and did, occur during 1995–1999 at Soufrière Hills Volcano. Although the details surrounding each individual dome collapse can vary significantly, some generalizations can be made. To facilitate this, dome-collapse phenomena have been categorized into three generic types (Table 4).

Passively generated rockfalls

Passively generated rockfalls occurred during periods of low activity (slow dome growth) and were associated with inactive flanks and older carapace material, and not with active shear lobes or headwalls. Comminution was less complete, and fewer fines were generated. Source material was thus probably largely degassed and spontaneous fragmentation of vesicular rock was not so active. Rockfall runout was therefore limited, with rockfalls rarely reaching past the break in slope at the base of the dome talus. At Montserrat, dome growth appears to have been mainly exogenous (Watts *et al.* 2002) but these rockfalls produced by collapse of unstable, largely degassed, carapace material may be comparable to the small-scale collapses produced by endogenous growth, as recognized by Ui *et al.* (1999).

Actively generated collapses (rockfalls and pyroclastic flows)

Most dome collapses (rockfalls and pyroclastic flows) were generated from actively growing portions of the dome, or shear-lobe headwalls. Rockfalls that were actively generated were commonly voluminous due to rapid development of large, metastable, oversteepened areas associated with rapid growth in a localized region of the dome. Larger collapses also occurred due to the inherently greater instability of the lava mass, and the tendency of the failure to progressively grow in volume. Where substrate slope changed, as at the edge of English's Crater, or over the edge of the old Castle Peak Dome, lobe fronts became inherently unstable and generated numerous rockfalls and pyroclastic flows. Periods when actively generated rockfalls were prevalent (e.g. May 1997; Fig. 5) were more often associated with the formation of longer-runout pyroclastic flows (when sufficiently large volumes of material were involved). Pyroclastic flows are therefore visualized as the larger-volume equivalent of actively generated rockfalls, as it was consistently from this activity that the longer runout (>1 km) pyroclastic flows were generated.

There is evidence that most, but not all, large to major dome collapses at Montserrat were related to pulses in extrusion rate. Dome extrusion rates were 4–6 $m^3 s^{-1}$ in the two or three days before the 29 July 1996 collapse and most other large to major collapses were preceded by one to five days of enhanced dome-growth rates (Table 1: e.g. December–January 1997 collapses; 25 June 1997; 3 August 1997). This is established by volumetric data for some cases (Figs 7 and 10), and interpreted indirectly for others; for example, by changes in tilt or by the onset of intense swarms of hybrid earthquakes. For much of the eruption, the occurrence of hybrid earthquakes appears to have been directly associated with the onset of instability of the lava dome. The tilt data identify significant pressure pulses spaced five to seven weeks apart, with the best examples beginning 22 June 1997 (just prior to the 25 June collapse) and 31 July 1997 (Voight *et al.* 1999). The timing of several other collapses (e.g. 21 September, 4 November and 26 December 1997) also fit this pattern, although tilt data were then unavailable. The tilt cycles have been interpreted in terms of shallow pressurization (<0.6 km below the base of the dome), at a position in the conduit influenced by a dramatic rise in magma melt viscosity. The change in viscosity is believed to be related to melt degassing and microlite crystallization (Sparks 1997; Voight *et al.* 1998, 1999; Melnik & Sparks 1999; Sparks *et al.* 2000). The hybrid earthquakes are further indicators of shallow pressurization, but require a threshold value of pressure. The pressure rise causes an eventual extrusion of a slug of magma, pressure is relieved in the upper conduit, and deflation occurs. Analysis of rockfall seis- mic records (Luckett *et al.* 2002) provides further evidence that actively generated rockfalls are intimately coupled with degassing of the dome. Vigorous hybrid earthquake swarms can also provoke rockfall activity by directly shaking the edifice. This mechanism is conzsidered as a minor, but recognizable, contributor to lava-dome instability during dome-growth periods.

Table 4. *Summary of dome-collapse phenomena*

	Passively generated rockfalls	Actively generated collapses	Post-extrusion collapses
Factors leading to collapse			
Locus on dome of collapse	Distributed on cold carapace	Shear lobes and push-up zones	Unstable areas
Extrusion rate prior to collapse	0–2 $m^3 s^{-1}$	>2 $m^3 s^{-1}$	0 $m^3 s^{-1}$
Apparent role of rainfall	May provoke rockfalls	Possible effect (rarely)	Provokes collapse in some cases
Gas content of material	Largely degassed	Gas-rich	Degassed carapace, gas-rich core
Volume of collapse	$<10^3$ m^3	10^3–10^7 m^3	10^3–10^7 m^3
Relation to tilt cycles and/or hybrid earthquakes	Not directly related but may be provoked by shaking	Commonly associated	No precursory seismic activity or crater-rim deformation
Ash-venting	Not observed	Following collapse (rarely)	Following collapse (commonly)
Explosive component	Not observed	In some cases associated with pulses of gas-rich magma	In some cases
Characteristics of flows			
Runout	<0.5 km	0.5–7 km	0.5–7 km
Degree of fragmentation	Fine ash poor	Fine ash rich	Fine ash rich
Flow types	Slow grain flows	Small pyroclastic flows to violent pyroclastic density currents	Small pyroclastic flows to major dome collapses associated with violent pyroclastic surges

Given the Soufrière Hills Volcano extrusion rates of 1–13 $m^3 s^{-1}$, and dome volumes that reached up to 113×10^6 m^3 during the 1995–99 period, most collapses of the lava dome removed no more than 18% of the dome (Fig. 8). The volumes of collapses, and the morphologies of the scoop-shaped scars they created, may have been influenced by the volume and structure of shear lobes. Shear lobe volumes were commonly in the range 10^5–10^6 m^3 (Watts *et al.* 2002), and therefore comparable to that of most medium to large dome collapses. Rockfall counts, amplitude and duration data (as determined seismically) reflect extrusion rate and growth locus variations and can thus be used (together) as a proxy for extrusion rate (Figs 9–11).

A few large to major dome collapses present exceptions. The 17 September 1996 and 26 December 1997 collapses were both exceptionally large (collapse of 35 and 50 vol% of the dome respectively), reflecting more complex generation mechanisms. The 17 September 1996 collapse volume included lava excavated from the crater during the subsequent sub-Plinian explosive activity (Fig. 6c; Robertson *et al.* 1998). The 26 December 1997 collapse was generated by failure of the hydrothermally altered wall of English's Crater, and the volume of dome rock and dome talus involved in this complex failure were 25×10^6 m^3 and 30×10^6 m^3 respectively (Sparks *et al.* 2002; Table 1). The 30 March and 11 April 1997 collapses were unusual in that they occurred during relatively low extrusion rates (<3 $m^3 s^{-1}$) although they were clearly related to shear-lobe extrusion. These events were also associated with the overtopping and partial destruction of Galway's Wall, and growth of the lobe headwall over the weakened, erodible, steep crater rim.

The distinction between passively and actively generated rockfalls leads to insights into the factors responsible for the generation of pyroclastic flows from fragmentation of the collapsing lava. Shear-lobe headwalls provide a rapidly replenished source of fresh lava only hours to days old, in a localized steep region. Within actively generated rockfalls the comminution is more complete, and this probably reflects the spontaneous disintegration of gas-pressurized vesicles and cracks. This is consistent with observations of autobrecciation, which suggest that wholesale fragmentation occurs when a pervasively microfractured rock-mass with over-pressurized pore space is critically stressed. The excavation level of collapse within the dome core is also of primary importance in the degree of fragmentation and in the subsequent generation of pyroclastic surges and buoyant ash plumes by rapid expansion of gases within the collapsing material (Voight & Elsworth 2000; Woods *et al.* 2002).

Further insights into the mechanism of spontaneous disintegration proposed for Montserrat are given by shock-tube fragmentation experiments on crystal-rich andesite. Such experiments suggest three fragmentation mechanisms – elastic unloading, a fragmentation wave and gas-filtration flow – which can contribute, depending on lava structure and decompression style, to the fragmentation of the magma (Alidibirov & Dingwell 2000). Experiments on Merapi Volcano (Indonesia) andesite at temperatures of 100–900°C and pressures up to 20 MPa show that the degree and character of fragmentation are controlled by density, crystal content and vesicle shape and distribution, with gas permeability the most important physical parameter (Spieler & Dingwell 1998).

Post-extrusion collapses

The collapses that occurred during the period of residual volcanic activity, after dome growth had ceased in March 1998 and before it commenced again in November 1999, present contrasting collapse mechanisms. The large collapses of 3 July 1998, 5 and 12 November 1998 and 20 July 1999 were preceded by neither hybrid earthquake swarms nor by crater-rim deformation. These collapses were associated with massive destruction of steep portions of the old, partially hydrothermally altered dome and they are distinctively different phenomena from the collapses associated with dome growth that are the main subject of this paper. The collapses initiated suddenly (Fig. 4), without build-up of rockfall events or other seismicity in the preceding minutes or hours. The onset of the seismic signals of some of these collapses (e.g. 3 July and 12 November 1998) has long-period components, suggesting a possible explosive triggering component. Unfortunately, visual confirmation of an explosive character is not available, although for the 12 November 1998 collapse, pyroclastic flows were produced simultaneously in three valleys. These collapses were also characterized by periods of intense degassing or ash-venting in the hours following collapse. The degree to which gas pressure build-up within the dome plays a role in their generation mechanisms is not yet well constrained. In these cases, however, it seems that gravitational instability of the precipitous rock walls, coupled with introduced gas pressure, was sufficient to produce flow deposits as voluminous as $20–25 \times 10^6$ m^3, and associated pyroclastic surges that inundated areas of >6 km^2. Especially heavy rainfall occurred before and during the collapse of 3 July 1998 (Norton *et al.* 2002), and this has been recognized elsewhere as an important collapse-triggering mechanism (Yamasato *et al.* 1998; Ratdomopurbo & Poupinet 2000; Voight *et al.* 2000b). Although rainfall-triggered collapses may also occur during active growth periods, they are likely to represent a more important mechanism during the months to years following cessation of extrusion.

These different collapse types currently fall under the broad term 'gravitational collapse'. At Montserrat, passively generated rockfalls, to some extent like post-extrusion collapses, occurred by development of internal weaknesses or pressure build-up, in situ, until the point at which gravity collapse could take over. Conversely, actively generated collapses were pushed to the point at which gravitational collapse could take over. The generation of pyroclastic flows (runout $\gg$0.5 km) from the collapsing material was determined by collapse of sufficiently large volumes of readily fragmented material either by actively generated collapse or during post-extrusion collapses.

Conclusions

We have investigated: (1) the factors that lead to instability of a lava dome, and that facilitate or trigger collapse episodes; and (2) how these characteristics promote the formation of rockfalls and pyroclastic flows.

Rockfall or pyroclastic flow generation by collapse of unstable portions of the growing lava dome occurred on an almost daily basis from March 1996 to March 1998. Large to major (>10^6 m^3) dome collapses began to occur once the volume of extruded andesite exceeded 30×10^6 m^3.

Large to major pyroclastic flows were generated during periods of elevated extrusion rate (6–13 $m^3 s^{-1}$), repetitive hybrid swarms, and cyclic crater-rim ground deformation. Material was shed from the dome at the onset of each deflation cycle, soon after a slug of magma (typically *c.* 250 000 m^3) had been extruded into the base of the dome. Most large to major collapses were produced after eight to 15 inflation–deflation cycles, but did not usually remove more than 18 vol% of the dome.

To a first order, the volume of material involved in a collapse depends on the volume of the dome. The time-averaged rate of lava extrusion for Montserrat was typically on the order 4–7 $m^3 s^{-1}$. For this range of extrusion rates, a log-linear relationship has been established for frequency versus magnitude of pyroclastic flows (using runout as a proxy for magnitude) and rockfalls (using event duration as a proxy for magnitude). The frequency data suggest a deficiency in recording of flows with 0.5–1 km runout.

The characteristics of lava extrusion are determined by extrusion rate, which can vary from week to week, and cyclic activity that can occur several times a day. For much of the eruption, lava has been extruded in shear lobes, which have played an important structural role in the generation of rockfalls and pyroclastic flows. The direction of the extruding lobe, and the location of the active headwall, have controlled the locations and directions of subsequent collapses. The timings of lobe extrusion determined variations in

rockfall and pyroclastic flow activity, both on a month-to-month scale and within individual hour-scale cycles. Collapse volumes and collapse-scar shape were probably also controlled by lobe structures. Importantly, active shear lobes provided the source material of pyroclastic flows, where material was hot and gas-rich, and disintegration of the microvesicular andesite lava occurred readily.

Collapse events occurring since the cessation of dome growth in March 1998, during the period of 'residual volcanic activity' (i.e. 3 July 1998, 5 and 12 November 1998 and 20 July 1999), were not related to extrusion rate or to shear-lobe formation, nor were they apparently associated with precursory seismic activity or ground deformation. In this case, catastrophic failures occurred from steep, eroded canyon-like walls, along inherent weakness planes, and were possibly triggered by environmental factors (rainfall) and facilitated by diffusing gas pressure within the dome. Seismic evidence suggests that there may have been an impulsive onset to some of these events, so that the assumption of a fully passive, gravity-driven collapse mechanism may not always be appropriate for these post-extrusion collapses.

MVO is supported by the UK Government (Department for International Development) and the Government of Montserrat. E.S.C. was supported by a NERC studentship GT4/95/35/E while at the University of Bristol. R.S.J.S. was supported by a NERC fellowship. The participation of B.V. was partly supported by NSF. We thank staff at the MVO who were responsible for the daily processing of the seismic data, in particular V. Bass. M. James is thanked for drafting the original version of Figure 6c, and G. Thomson for resolving a number of problems regarding seismic data. Reviews by C. Newhall and S. Nakada and thorough editing by T. Druitt helped to improve the manuscript.

References

Abdurachman, E. K., Bourdier, J. L. & Voight, B. 2000. Nuées ardentes of November 22 1994 at Merapi Volcano, Indonesia. *Journal of Volcanology and Geothermal Research*, **100**, 345–361.

Alidibirov, M. & Dingwell, D. B. 2000. Three fragmentation mechanisms for highly viscous magma under rapid decompression. *Journal of Volcanology and Geothermal Research*, **100**, 413–421.

Anderson, T. & Flett, J. S. 1903. Report on the eruptions of the Soufrière St. Vincent, in 1902, and on a visit to Montagne Pelée, in Martinique – Part 1. *Philosophical Transactions of the Royal Society London*, **A-200**, 353–553.

Aspinall, W. P., Miller, A. D., Lynch, L. L., Latchman, J. L., Stewart, R. C., White, R. A. & Power, J. A. 1998. Soufrière Hills eruption, Montserrat 1995–1997: Volcanic earthquake locations and fault plane solutions. *Geophysical Research Letters*, **25**, 3397–3400.

Barclay, J., Rutherford, M. J., Carroll, M. R., Murphy, M. D., Devine, J. D., Gardner, J. & Sparks, R. S. J. 1998. Experimental phase equilibria constraints on pre-eruptive storage conditions of the Soufrière Hills magma. *Geophysical Research Letters*, **25**, 3437–3440.

Bonadonna, C., Mayberry, G. C., Calder, E. S. *et al.* 2002. Tephra fallout in the eruption of Soufrière Hills Volcano, Montserrat. *In:* Druitt, T. H. & Kokelaar, B. P. (eds) *The Eruption of Soufrière Hills Volcano, Montserrat, from 1995 to 1999*. Geological Society, London, Memoirs, **21**, 483–516.

Boudon, G., Camus, G., Gourgaud, A. & Lajoie, J. 1993. The 1984 nuée-ardente deposits of Merapi Volcano, Central Java, Indonesia: Stratigraphy, textural characteristics and transport mechanisms. *Bulletin of Volcanology*, **55**, 327–342.

Brodscholl, A. L., Kirbani, S. B. & Voight, B. 2000. Sequential dome-collapse nuées ardentes analysed from broadband seismic data, Merapi Volcano, Indonesia. *Journal of Volcanology and Geothermal Research*, **100**, 363–369.

Calder, E. S. 1999. *Dynamics of small to intermediate volume pyroclastic flows*. PhD Thesis, University of Bristol.

Calder, E. S., Cole, P. D., Dade, W. B. *et al.* 1999. Mobility of pyroclastic flows and surges at the Soufrière Hills Volcano, Montserrat. *Geophysical Research Letters*, **26**, 537–540.

Chouet, B. A. 1996 Long-period volcano seismicity – its source and use in eruption forecasting. *Nature*, **380**, 309–316.

Clarke, A. B., Neri, A., Voight, B., Macedonio, G. & Druitt, T. H. 2002. Computational modelling of the transient dynamics of August 1997 Vulcanian explosions at Soufrière Hills Volcano, Montserrat: influence of initial conduit conditions on near-vent pyroclastic dispersal. *In:* Druitt, T. H. & Kokelaar, B. P. (eds) *The Eruption of Soufrière Hills Volcano, Montserrat, from 1995 to 1999*. Geological Society, London, Memoirs, **21**, 319–348.

Cole, P. D., Calder, E. S., Druitt, T. H., Hoblitt, R., Robertson, R. E. A., Sparks, R. S. J. & Young, S. R. 1998. Pyroclastic flows generated by gravitational instability of the 1996–97 lava dome of the Soufrière Hills Volcano, Montserrat. *Geophysical Research Letters*, **25**, 3425–3428.

Cole, P. D., Calder, E. S., Sparks, R. S. J. *et al.* 2002. Deposits from dome-collapse and fountain-collapse pyroclastic flows at Soufrière Hills Volcano, Montserrat. *In*: Druitt, T. H. & Kokelaar, B. P. (eds) *The Eruption of Soufrière Hills Volcano, Montserrat, from 1995 to 1999*. Geological Society, London, Memoirs, **21**, 231–262.

Dade, W. B. & Huppert, H. E. 1998. Long runout rockfalls. *Geology*, **26**, 803–806.

Druitt, T. H., Calder, E. S., Cole, P. D. *et al.* 2002*a*. Small-volume, highly mobile pyroclastic flows formed by rapid sedimentation from pyroclastic surges at Soufrière Hills Volcano, Montserrat: an important volcanic hazard. *In*: Druitt, T. H. & Kokelaar, B. P. (eds) *The Eruption of Soufrière Hills Volcano, Montserrat, from 1995 to 1999*. Geological Society, London, Memoirs, **21**, 263–279.

Druitt, T. H., Young, S. R., Baptie, B. *et al.* 2002*b*. Episodes of cyclic Vulcanian explosive activity with fountain collapse at Soufrière Hills Volcano, Montserrat. *In*: Druitt, T. H. & Kokelaar, B. P. (eds) *The Eruption of Soufrière Hills Volcano, Montserrat, from 1995 to 1999*. Geological Society, London, Memoirs, **21**, 281–306.

Endo, E. T. & Murray, T. L. 1991. Real-time seismic amplitude measurement (RSAM), a volcano monitoring and prediction tool. *Bulletin of Volcanology*, **53**, 533–545.

Escher, B. G. 1933. On a classification of central eruptions according to gas pressure of the magma and viscosity of the lava. *Leidsche Geologische Mededeelingen*, **6**, 45–49.

Fink, J. H. & Kieffer, S. W. 1993. Estimates of pyroclastic flow velocities from explosive decompression of lava domes. *Nature*, **363**, 612–615.

Fisher, R. V. 1995. Decoupling of pyroclastic currents: hazards assessment. *Journal of Volcanology and Geothermal Research*, **66**, 257–263.

Grunewald, U., Sparks, R. S. J., Kearns, S. & Komorowski, J.-C. 2000. Friction marks on blocks from pyroclastic flows at the Soufrière Hills volcano, Montserrat: implications for flow mechanisms. *Geology*, 28, 827–830.

Lacroix, A. 1904. *La Montagne Pelée et ses eruptions*. Masson et cie, Paris.

Loughlin, S. C., Baxter, P. J., Aspinall, W. P., Darroux, B., Harford, C. L. & Miller, A. D. 2002*a*. Eyewitness accounts of the 25 June 1997 pyroclastic flows and surges at Soufrière Hills Volcano, Montserrat, and implications for disaster mitigation. *In:* Druitt, T. H. & Kokelaar, B. P. (eds) *The Eruption of Soufrière Hills Volcano, Montserrat, from 1995 to 1999*. Geological Society, London, Memoirs, **21**, 211–262.

Loughlin, S. C., Calder, E. S., Clarke, A. B. *et al.* 2002*b*. Pyroclastic flows and surges generated by the 25 June 1997 dome collapse, Soufrière Hills Volcano, Montserrat. *In*: Druitt, T. H. & Kokelaar, B. P. (eds) *The Eruption of Soufrière Hills Volcano, Montserrat, from 1995 to 1999*. Geological Society, London, Memoirs, **21**, 191–209.

Luckett, R., Baptie, B. & Neuberg, J. 2002. The relationship between degassing and rockfall signals at Soufrière Hills Volcano, Montserrat. *In*: Druitt, T. H. & Kokelaar, B. P. (eds) *The Eruption of Soufrière Hills Volcano, Montserrat, from 1995 to 1999*. Geological Society, London, Memoirs, **21**, 595–602.

Mellors, R. A., Waitt, R. B. & Swanson, D. A. 1988. Generation of pyroclastic flows and surges by hot-rock avalanches from the dome of Mount St. Helens Volcano, USA. *Bulletin of Volcanology*, **50**, 14–25.

Melnik, O. & Sparks, R. S. J. 1999. Nonlinear dynamics of lava dome extrusion. *Nature*, **402**, 37–41.

Miller, A. D., Stewart, R. C., White, R. A. *et al.* 1998. Seismicity associated with dome growth and collapse at the Soufrière Hills Volcano, Montserrat. *Geophysical Research Letters*, **25**, 3401–3404.

Murphy, M. D., Sparks, R. S. J., Barclay, J. *et al.* 1998. The role of magma mixing in triggering the current eruption at the Soufrière Hills Volcano, Montserrat, West Indies. *Geophysical Research Letters*, **25**, 3433–3436.

MURPHY, M. D., SPARKS, R. S. J., BARCLAY, J., CARROLL, M. R. & BREWER, T. S. 2000. Remobilisation origin for andesite magma by intrusion of mafic magma at the Soufrière Hills Volcano, Montserrat, W. I., a trigger for renewed eruption. *Journal of Petrology*, **41**, 21–42.

NAKADA, S. & FUJII, T. 1993. Preliminary report on the activity at Unzen Volcano (Japan), November 1990–November 1991: Dacite lava domes and pyroclastic flows. *Journal of Volcanology and Geothermal Research*, **54**, 319–333.

NAKADA, S., SHIMIZU, H. & OHTA, K. 1999. Overview of the 1990–1995 eruption at Unzen Volcano. *Journal of Volcanology and Geothermal Research*, **89**, 1–22.

NEUBERG, J. 2000. Characteristics and causes of shallow seismicity in andesite volcanoes. *Philosophical Transactions of the Royal Society of London*, **A358**, 1533–1546.

NEUBERG, J., BAPTIE, B., LUCKETT, R. & STEWART, R. 1998. Results from the broadband seismic network on Montserrat. *Geophysical Research Letters*, **25**, 3661–3664.

NEWHALL, C. G. & MELSON, W. G. 1982. Explosive activity associated with the growth of volcanic domes. *Journal of Volcanology and Geothermal Research*, **17**, 111–131.

NORRIS, R. D. 1994. Seismicity of rockfalls and avalanches at three Cascade Range volcanoes: Implications for seismic detection of hazardous mass movements. *Bulletin of the Seismology Society of America*, **84**, 1925–1939.

NORTON, G. E., WATTS, R. B., VOIGHT, B. *ET AL.* 2002. Pyroclastic flow and explosive activity at Soufrière Hills Volcano, Montserrat, during a period of virtually no magma extrusion (March 1998 to November 1999). *In*: DRUITT, T. H. & KOKELAAR, B. P. (eds) *The Eruption of Soufrière Hills Volcano, Montserrat, from 1995 to 1999*. Geological Society, London, Memoirs, **21**, 467–481.

PERRET, F. A. 1937. *The eruption of Mt. Pelée 1929–1932*. Carnegie Institute, Washington, Publication No. **458**.

RATDOMOPURBO, A. & POUPINET, G. 2000. An overview of the seismicity of Merapi volcano (Java, Indonesia) 1983–1994. *Journal of Volcanology and Geothermal Research*, **100** 193–214.

RITCHIE, L. J., COLE, P. D. & SPARKS, R. S. J. 2002. Sedimentology of deposits from the pyroclastic density current of 26 December 1997 at Soufrière Hills Volcano, Montserrat. *In*: DRUITT, T. H. & KOKELAAR, B. P. (eds) *The Eruption of Soufrière Hills Volcano, Montserrat, from 1995 to 1999*. Geological Society, London, Memoirs, **21**, 435–456.

ROBERTSON, R. E. A., COLE, P. D., SPARKS, R. S. J. *ET AL.* 1998. The explosive eruption of Soufrière Hills Volcano, Montserrat, 17 September 1996. *Geophysical Research Letters*, **25**, 3429–3432.

RODRIGUEZ-ELIZARRARAS, S., SIEBE, C., KOMOROWSKI, K-C, ESPIDOLA, J. M. & SAUCEDO, R. 1991. Field observations of pristine block-and-ash flow deposits emplaced April 16–17 1991 at Volcan Colima, Mexico. *Journal of Volcanology and Geothermal Research*, **48**, 399–412.

ROSE, W. I., PEARSON, T. & BONIS, S. 1977. Nuée ardent eruption from the foot of a dacite lava flow, Santiaguito Volcano, Guatemala. *Bulletin of Volcanology*, **40**, 23–38.

SATO, H., FUJII, T. & NAKADA, S. 1992. Crumbling dacite dome lava and generation of pyroclastic flows at Unzen Volcano. *Nature*, **360**, 664–666.

SPARKS, R. S. J. 1997. Causes and consequences of pressurisation in lava dome eruptions. *Earth and Planetary Science Letters*, **150**, 177–189.

SPARKS, R. S. J., YOUNG, S. R., BARCLAY, J. *ET AL.* 1998. Magma production and growth of the lava dome of the Soufrière Hills Volcano, Montserrat, West Indies: November 1995 to December 1997. *Geophysical Research Letters*, **25**, 3421–3424.

SPARKS, R. S. J., MURPHY, M. D., LEJEUNE, A. M., WATTS, R. B., BARCLAY, J. & YOUNG, S. R. 2000. Control on the emplacement of the andesite lava dome of the Soufrière Hills Volcano, Montserrat by degassing-induced crystallization. *Terra Nova*, **12**, 14–20.

SPARKS, R. S. J., BARCLAY, J., CALDER, E. S. *ET AL.* 2002. Generation of a debris avalanche and violent pyroclastic density current on 26 December (Boxing Day) 1997 at Soufrière Hills Volcano, Montserrat. *In*: DRUITT, T. H. & KOKELAAR, B. P. (eds) *The Eruption of Soufrière Hills Volcano, Montserrat, from 1995 to 1999*. Geological Society, London, Memoirs, **21**, 409–434.

SPIELER, O. & DINGWELL, D. B. 1998. Experimental fragmentation of vesicular basaltic andesite from Merapi (abstract). AGU 79, No 45.

UHIRA, K., YAMASATO, M. & TAKEO, M. 1994. Source mechanism of seismic waves excited by pyroclastic flows observed at Unzen volcano, Japan. *Journal of Geophysical Research*, **99**, 17 757–17 773.

UI, T., MATSUWO, N., SUMITA, M. & FUJINAWA, A. 1999. Generation of block and ash flows during the 1990–1995 eruption of Unzen Volcano, Japan. *Journal of Volcanology and Geothermal Research*, **89**, 123–137.

VOIGHT, B. & ELSWORTH, 2000. Instability and collapse of gas-pressurised lava domes. *Geophysical Research Letters*, **27**, 1–4.

VOIGHT, B., HOBLITT, R. P., CLARKE, A. B., LOCKHART, A. B., MILLER, A. D., LYNCH, L. & MCMAHON, J. 1998. Remarkable cyclic ground deformation monitored in real-time on Montserrat, and its use in eruption forecasting. *Geophysical Research Letters*, **25**, 3405–3408.

VOIGHT, B., SPARKS, R. S. J., MILLER, A. D. *ET AL.* 1999. Magma flow instability and cyclic activity at Soufriere Hills Volcano, Montserrat, British West Indies. *Science*, **283**(5405) 1138–1142.

VOIGHT, B., YOUNG, K. D., HIDAYAT, D. *ET AL.* 2000*a*. Deformation and seismic precursors to dome-collapse and fountain-collapse nuées ardentes at Merapi Volcano, Indonesia 1994–1998. *Journal of Volcanology and Geothermal Research*, **100,** 261–287.

VOIGHT, B., CONSTANTINE, E. K., SISWOWIDJOYO, S. & TORLEY, R. 2000*b* Historical eruptions of Merapi Volcano, Central Java, Indonesia, 1768–1998. *Journal of Volcanology and Geothermal Research*, **100**, 69–138.

WATTS, R. B., HERD, R. A., SPARKS, R. S. J. & YOUNG, S. R. 2002. Growth patterns and emplacement of the andesitic lava dome at Soufrière Hills Volcano, Montserrat. *In*: DRUITT, T. H. & KOKELAAR, B. P. (eds) *The Eruption of Soufrière Hills Volcano, Montserrat, from 1995 to 1999*. Geological Society, London, Memoirs, **21**, 115–152.

WOODS, A. & KIENLE, J. 1994. The dynamics and thermodynamics of volcanic clouds: theory and observations from the April 15 and April 21, 1990 eruptions of Redoubt Volcano, Alaska. *Journal of Volcanology and Geothermal Research*, **62**, 273–299.

WOODS, A. W., SPARKS, R. S. J., RITCHIE, L. J., BATEY, J., GLADSTONE, C. & BURSIK, M. 2002. The explosive decompression of a pressurized lava dome: the 26 December 1997 collapse and explosion of Soufrière Hills Volcano, Montserrat. *In*: DRUITT, T. H. & KOKELAAR, B. P. (eds) *The Eruption of Soufrière Hills Volcano, Montserrat, from 1995 to 1999*. Geological Society, London, Memoirs, **21**, 457–466.

YAMAMOTO, T., TAKARADA, S. & SUTO, S. 1993. Pyroclastic flows from the 1991 eruption of Unzen Volcano, Japan. *Bulletin of Volcanology*, **55**, 166–175.

YAMASATO, H., KITAGAWA, S. & KOMIYA, M. 1998. Effect of rainfall on dacitic lava dome collapse at Unzen volcano, Japan. *Papers in Meterology and Geophysics*, **48**(3), 73–78 [in Japanese].

YOUNG, S. R., SPARKS, R. S. J., ASPINALL, W. P., LYNCH, L. L., MILLER, A. D., ROBERTSON, R. E. A. & SHEPHERD, J. B. 1998. Overview of the eruption of Soufrière Hills Volcano, Montserrat, 18 July 1995 to December 1997. *Geophysical Research Letters*, **25**(18), 3389–3392.